

Historical biogeography of Middle-East mangroves: paleobotanical evidence

Valentí Rull

Paleoecological Research (PaleoRes), Barcelona, Spain. Email: rullv@paleores.org

Abstract

This paper reconstructs the origin, diversification, and decline of Middle East (ME) mangroves from the Late Cretaceous to the present using the MESMA database, a comprehensive compilation of fossil pollen and macrofossil records integrated with paleogeographic, tectonic, climatic and sea-level evidence. To date, global paleobiogeographical and evolutionary syntheses of mangroves have emphasized the role of the ME region as either a dispersal corridor or a biogeographical barrier, rather than as a research focus in its own right. The earliest reliable ME mangrove records correspond to *Nypa* from the Late Cretaceous, when the present-day Arabian Peninsula formed part of the Nubian Plate along the southern Tethyan margin. A potential Albian precursor suggests that the ME may have played a role in the early evolution of the *Nypa* lineage, which, if confirmed, would represent the earliest mangrove record worldwide. Mangrove diversification began in the Eocene with the arrival of *Avicennia* and *Acrostichum*, followed by *Rhizophora* in the Oligocene, leading to the highest diversity levels recorded in the region. This diversification is remarkable because it occurred during the Eocene/Oligocene transition, a phase associated with mangrove decline in most other parts of the world. A major biodiversity crisis took place during the Middle Miocene, when regional desertification associated with the Middle Miocene Climatic Transition, likely linked to the Arabia–Eurasia collision and the resulting closure of the Tethys Sea, caused the disappearance of most mangrove elements, leaving only *Avicennia* and *Rhizophora* as surviving mangrove-forming taxa. This event established the low-diversity pattern that characterizes present-day ME mangroves. Quaternary records are scarce, but Holocene sequences from southern Arabia document a pronounced reduction of *Rhizophora* between approximately 6.5 and 4.5 ka BP, coinciding with the termination of the Holocene Humid Period, after which the genus survived only in a few relict areas, whereas the more stress-tolerant *Avicennia* persisted and became dominant. In contrast to previous studies, this synthesis identifies the ME as a significant region for mangrove evolution per se, rather than merely in relation to other biogeographical regions. The study also highlights substantial gaps in the fossil record and several unresolved questions that provide promising avenues for future research.

Keywords

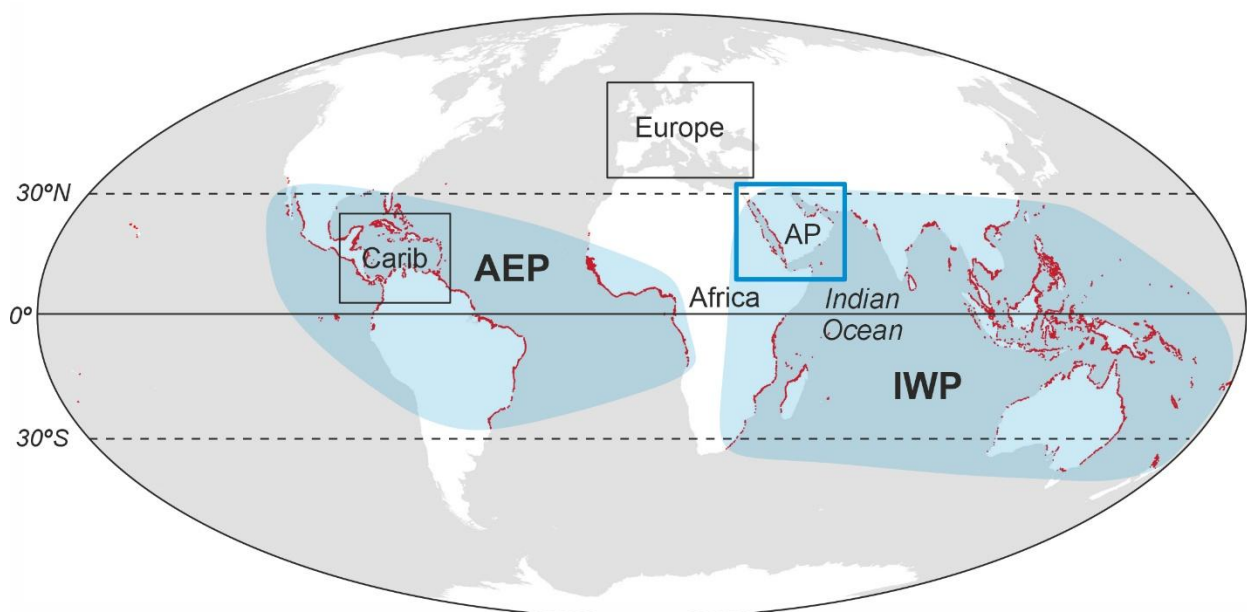
Mangroves, Middle East, biogeography, evolution, paleogeography, paleoclimates, plant fossils

53 1. Introduction

54
55 Mangroves are land–sea transitional forested wetland ecosystems that occupy the outer margin of all
56 continents, extending to the limit of normal tidal influence along tropical and subtropical coasts, roughly
57 between 30° N and 30° S worldwide (Spalding et al., 2010) (Fig. 1). They play an important role in coastal
58 protection and in sustaining both continental and marine biodiversity and ecosystem processes
59 (Nagelkerken et al., 2008). In addition, mangroves are significant contributors to global biogeochemical
60 cycles—particularly the carbon cycle—as a major blue carbon ecosystem that helps mitigate global
61 warming (Fest et al., 2022).

62 Mangrove forests are organized around a number of dominant mangrove-forming tree species –
63 known as major true-mangrove elements and exclusive to these communities – that define the physical
64 structure of the community, and without which mangrove ecosystems cannot persist (Table 1). These
65 mangrove-forming taxa exhibit specialized morphological and physiological adaptations that allow them
66 to tolerate intertidal conditions with soft, anoxic sediments and fluctuating water levels and salinity
67 (Tomlinson, 2016). These adaptations occurred at various evolutionary times across different unrelated
68 lineages, constituting one of the most striking cases of evolutionary convergence in the plant kingdom (Xu
69 et al., 2017; He et al., 2020). Minor true-mangrove elements are also exclusive to mangroves and exhibit
70 similar adaptations; however, they rarely form pure stands and typically occupy a marginal position within
71 the community.

72 Among mangrove-forming taxa, only *Rhizophora* (Rhizophoraceae) and *Avicennia* (Acanthaceae)
73 have a global distribution, although their species are disjunctly distributed across two major
74 biogeographical regions: the Atlantic–East Pacific (AEP) and the Indo–West Pacific (IWP), which are
75 separated by the African continental barrier (Tomlinson, 2016; Duke, 2017) (Fig. 1). The remaining
76 mangrove genera are confined either to the AEP or the IWP, with the exception of the fern genus
77 *Acrostichum* (Pteridaceae), which also has a cosmopolitan distribution. The IWP region, with 17 true-
78 mangrove genera and 54 species, is far more diverse than the AEP, which has only 6 genera and 11 species
79 (Table 1).
80



81
82
83 **Figure 1.** Worldwide mangrove distribution (red fringes) highlighting the Atlantic-East Pacific (AEP) and Indo-West Pacific (IWP)
84 biogeographical regions (blue shading). The study area is indicated by a blue box, while regions previously studied using the same
85 methodology (Europe and the Caribbean) are denoted by black boxes. AP, Arabian Peninsula. Base map from Rull (2022),
86 downloaded from <https://data.unep-wcmc.org/datasets/5> (last accessed April 15, 2026).
87
88
89
90

91 **Table 1.** Extant mangrove-forming tree genera distributed across global mangrove biogeographical regions, indicating the
 92 number of species present in each region (Tomlinson, 2016; Duke, 2017). Note the greater diversity in the IWP region (17 genera,
 93 54 species) compared to the EAP region (6 genera, 11 species). The genera included in this review, together with their
 94 corresponding fossil representatives, are marked with an asterisk. Note that only three of the major mangrove elements and two
 95 (or one, if *Pelliciera* is excluded) of the minor mangrove elements are represented. The fossil pollen *Proxapertites* (notably *P.*
 96 *operculatus* and *P. cursus*) has sometimes been linked to *Nypa*, but is now considered to belong to the Araceae (Zetter et al.,
 97 2001; Hesse & Zetter, 2007).
 98

Type	True-mangrove genera	extant	AEP	IWP	Fossil pollen/spore/macrofossil (P/S/M) representatives in the ME record
Major	<i>Rhizophora</i> (Rhizophoraceae)*		4	8	<i>Zonocostites ramonae</i> (P)
	<i>Avicennia</i> (Acanthaceae)*		3	5	<i>Avicennia</i> (P/M)
	<i>Laguncularia</i> (Combretaceae)		1		
	<i>Nypa</i> (Arecaceae)*			1	<i>Spinizonocolpites baculatus</i> (P), <i>S. prominatus</i> (= <i>S. echinatus</i>) (P), <i>Nypa</i> (M), <i>Nipadites</i> (M), <i>Rubiaceocarpum markgrafi</i> (M), <i>Apeibopsis gigantea</i> (M)
	<i>Lumnitzera</i> (Combretaceae)			3	
	<i>Bruguiera</i> (Rhizophoraceae)			7	
	<i>Ceriops</i> (Rhizophoraceae)			5	
	<i>Kandelia</i> (Rhizophoraceae)			2	
	<i>Sonneratia</i> (Sonneratiaceae)			9	
Minor	<i>Acrostichum</i> (Pteridaceae)*		1	2	<i>Deltoidospora adriennis</i> (S)
	<i>Conocarpus</i> (Combretaceae)		1		
	<i>Pelliciera</i> (Tetrameristaceae)* ¹		1		<i>Psilatricolporites crassus</i> (= <i>Lanagiopollis crassa</i>) (P)
	<i>Excoecaria</i> (Euphorbiaceae)			1	
	<i>Pemphis</i> (Lythraceae)			1	
	<i>Camptostemon</i> (Malvaceae)			2	
	<i>Xylocarpus</i> (Meliaceae)			2	
	<i>Osbornia</i> (Myrtaceae)			1	
	<i>Aegialitis</i> (Plumbaginaceae)			2	
	<i>Aegiceras</i> (Primulaceae)			2	
<i>Scyphiphora</i> (Rubiaceae)			1		

99 ¹Questioned in this work due to identification issues (Rull, 2025, 2026).
 100

101 The origin of these global biogeographical patterns has been explained by either dispersalist or
 102 vicariant processes. Dispersalist hypotheses propose that ancestral lineages originated in the more
 103 species-rich IWP region and later dispersed to the AEP region (Van Steenis, 1962), whereas vicariant
 104 models suggest that mangroves evolved during the Late Cretaceous along the margins of the tropical
 105 Tethys Sea and subsequently diversified following its closure due to the formation of the African barrier
 106 (McCoy and Heck, 1976; Ellison et al., 1999). Estimates for the timing of the IWP–AEP divergence differ
 107 widely among studies, ranging from the Late Cretaceous to the Oligocene (Ellison et al., 1999; Plaziat et
 108 al., 2001; Duke, 2017; Srivastava & Prasad, 2019). More recent molecular phylogeographical evidence
 109 suggests that both vicariance and long-distance dispersal are required to explain the present distribution
 110 of *Rhizophora* (Lo et al., 2014; Takayama et al., 2021), although the timing of speciation remains
 111 unresolved, with estimates spanning from the Eocene to the Miocene. While allopatric diversification
 112 associated with the closure of the Tethys Sea remains a widely accepted explanation across many plant

113 and animal groups (e.g., Celâl Şengör & Saniye, 2009; Zhao et al., 2022), the role of long-distance dispersal
114 is often underestimated (Van der Stocken et al., 2019).

115 The region commonly referred to as the Middle East, encompassing the Arabian Peninsula and
116 adjacent areas, occupies an intermediate geographical position between the EAP and the IWP (Fig. 1), but
117 biogeographically it belongs to the IWP. Both the Middle East and its mangroves are noteworthy for some
118 exceptional present and past biogeographical peculiarities. Extant mangroves from this region are
119 considered a biogeographical anomaly relative to those at similar latitudes elsewhere, owing to their
120 limited extent and low biodiversity resulting from extreme environmental conditions—primarily high
121 temperatures, aridity and hypersalinity (Osland et al., 2017; Meraj et al., 2025; Waleed et al., 2025). ME
122 mangroves have sometimes been considered potential modern analogs for mangroves inhabiting Europe
123 during the Middle Miocene Climatic Optimum (MMCO); however, their anomalous latitudinal nature does
124 not support such an assessment (Rull et al., 2026).

125 The region has also been identified as a key biogeographical corridor that served as the principal
126 pathway for the westward migration of IWP mangrove taxa during the Cenozoic, a process that was
127 fundamental in shaping European mangroves prior to the Oligocene closure of the passage between Africa
128 and Asia by the Arabian Peninsula (Rull, 2026). This peninsula was part of the African Plate prior to the
129 Africa–Asia collision (Macgregor & Reeves, 2025) and thus carried floristic elements of African origin.
130 Consequently, the closure of the Tethys seaway would have marked not only the loss of a dispersal
131 pathway for marine and coastal organisms but also the convergence of elements from three different
132 regions: IWP, Africa and western Asia.

133 Despite these singularities and their global significance, ME mangroves and their ancestors have
134 received little attention compared with other more extensive and diverse mangrove regions, notably the
135 Caribbean and Southeast Asia (Ward et al., 2016). This is especially true in fields such as evolutionary
136 biology, physiology and molecular biology (Friis & Burt, 2020). These authors identified the evolutionary
137 history of Middle East mangroves and their biogeographical relationships with other mangrove-bearing
138 regions—the main focus of this review—as an important knowledge gap that deserves further
139 investigation. To date, global mangrove paleobiogeographical and evolutionary syntheses have
140 emphasized the role of the Middle East region as either a dispersal pathway or a biogeographical barrier
141 for mangroves, rather than as a research target in its own right (e.g., Ellison et al., 1999; Morley, 2000;
142 Plaziat et al., 2001; Duke, 2017; Srivastava & Prasad, 2019). As a result, a spatiotemporal integrative
143 understanding of ME mangroves in terms of their origin, evolution and the acquisition of their current
144 taxonomic composition and biogeographical patterns is still lacking.

145 Recently, an initiative has been launched to investigate mangrove origin and development from
146 the Cretaceous to the present using palaeobotanical evidence as the primary proxy for mangrove
147 communities structured around mangrove-forming tree species. This effort focuses on biogeographically
148 significant mangrove-bearing regions worldwide. To date, comprehensive reviews are available for the
149 Caribbean region and Europe (Rull, 2024, 2026). This paper is the third in the series to apply the same
150 methodology, contributing toward a future integrated synthesis of mangrove origin and evolution at the
151 global scale. Indeed, the combination of CARMA (CARibbean MAngroves; Rull, 2024), EURMA (EUropean
152 MAngroves; Rull, 2026), and MESMA (Middle East MAngroves; this paper), together with other similar
153 datasets that may be developed in the future (for example WAFMA from Western Africa, which is in
154 progress, will provide a robust and comprehensive body of evidence for addressing global patterns of
155 mangrove evolution and biogeography without losing fine-grained detail, as these datasets are based on
156 primary, site-by-site fossil evidence.

157

158 **2. Study area**

159

160 *2.1. Geographical and geological setting*

161

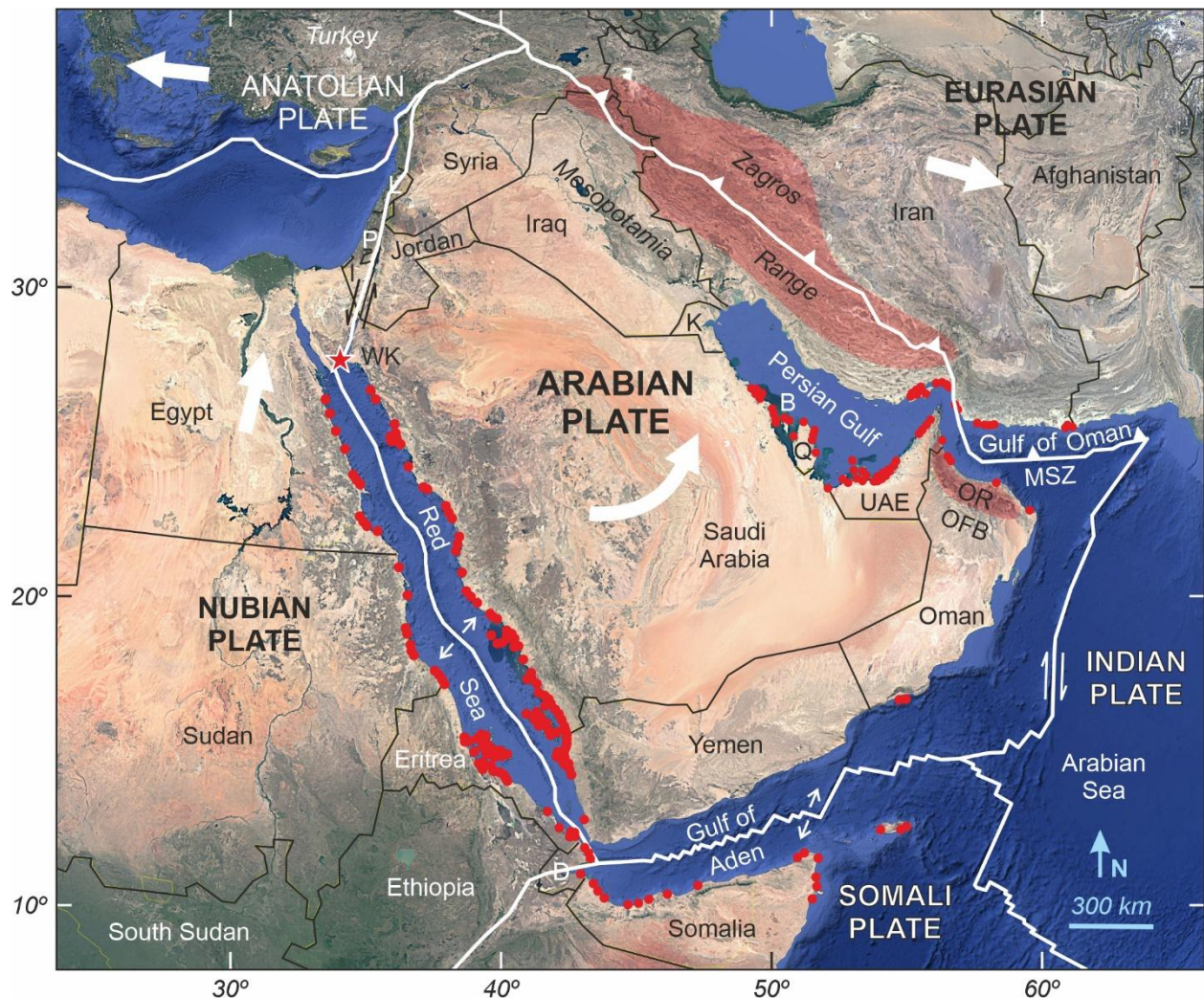
162 The area considered in this review extends approximately from 10° to 40° N latitude and 25° to 65° E
163 longitude (Fig. 2) and includes 21 countries: 6 in northeastern Africa (Djibouti, Ethiopia, Eritrea, Egypt,
164 Somalia and Sudan) and 14 in southwestern Asia (Bahrain, Iran, Iraq, Israel, Jordan, Kuwait, Lebanon,
165 Oman, Palestine, Qatar, Saudi Arabia, Syria, the United Arab Emirates and Yemen). Tectonically, this area

166 is defined by the complex interactions among the Arabian, African (Nubian and Somali), Eurasian, Indian
 167 and Anatolian plates.

168 Countries located in the northernmost part currently lack mangrove communities, but they are
 169 included in the study because they form part of the Arabian Plate, whose long-term dynamics are
 170 fundamental to understanding mangrove evolution in the region. Turkey was already included in the
 171 analysis of Cenozoic European mangroves, but the localities in its central and southern regions are also
 172 considered here because of their proximity to the junction of the Anatolian with the Arabian and Nubian
 173 plates.

174 Given the cultural (Eurocentric) connotations of the term “Middle East,” a more descriptive and
 175 neutral biogeographical designation for the study area—such as the northern sector of the Western Indo-
 176 Pacific coastal realm (Spalding et al., 2007), abbreviated as NWIP—may be preferable. An alternative is
 177 the purely geographical term “northwestern Indian Ocean (NWIO) coasts.” The traditional term “Middle
 178 East” (thereafter ME) is retained here to maintain consistency with existing literature and facilitate
 179 comparisons, although it may be revised in the future.

180

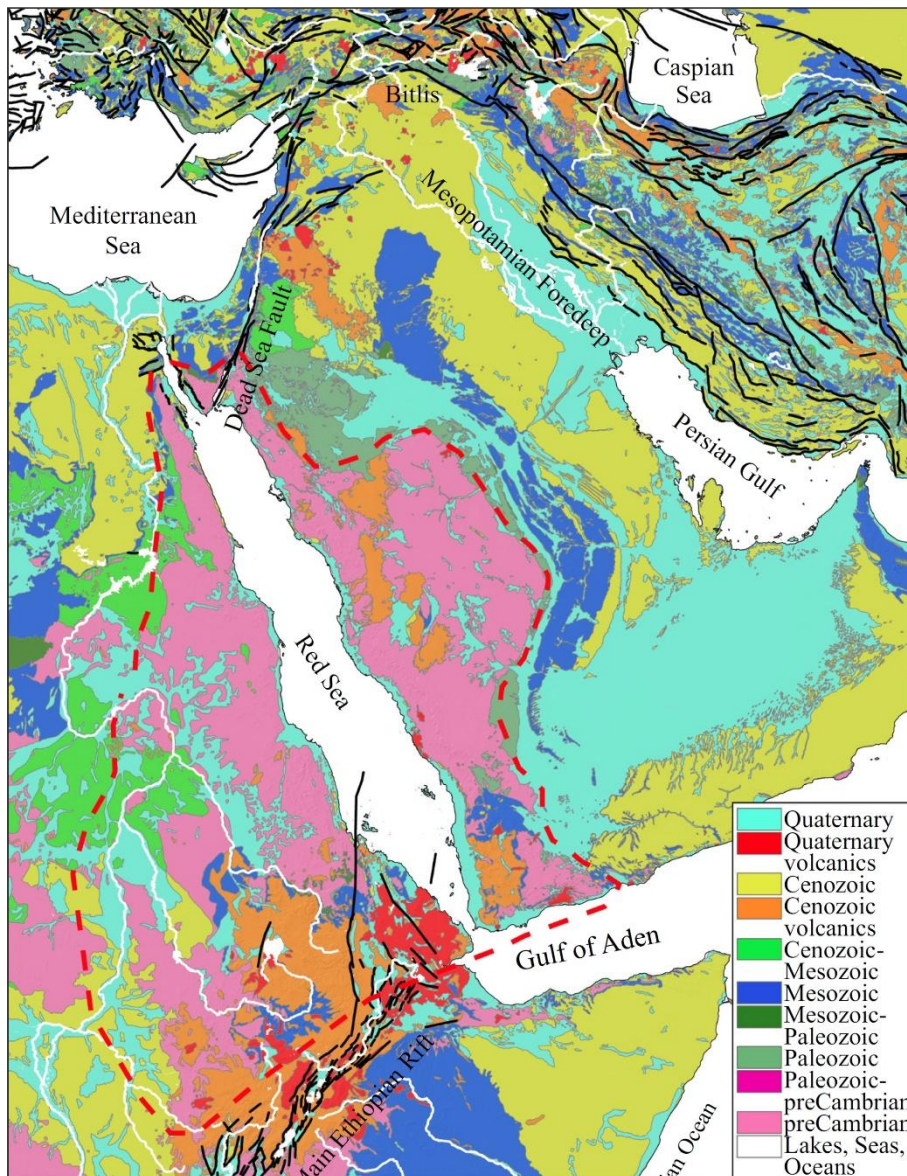


181
 182
 183 **Figure 2.** Detailed Google Earth map of the study area. Extant mangroves are represented as red dots/areas, redrawn from Meraj
 184 et al. (2025). Somalia occurrences according to Mohamed (2026). The northernmost mangrove (WK, Wadi Kid) is indicated by a
 185 star. Tectonic plates have been drawn with Google Earth using the corresponding layer from the US Geological Survey
 186 (downloaded from <https://www.usgs.gov/programs/earthquake-hazards/google-earth-tkml-files>;
 187 last accessed March 18, 2026). Details and plate motion vectors (white arrows) from Peña et al. (2022). Countries: B, Bahrain; D, Djibouti; I, Israel; K,
 188 Kuwait; L, Lebanon; P, Palestine; Q, Qatar; UAE, United Arab Emirates. Tectonic units (Oman): MSZ, Makran subduction zone;
 189 OFB, Oman foreland basin; OR, Oman Range.

190

191 The geology of the Middle East is dominated by a broad contrast between the stable Arabian Platform
 192 and the tectonically active mountain belts that border it to the north and northeast. Precambrian
 193 crystalline rocks of the Arabian–Nubian Shield are extensively exposed along the Red Sea margins and
 194 across western Saudi Arabia, forming the oldest geological foundation of the region (Fig. 3). These rocks
 195 are overlain eastward by widespread Paleozoic, Mesozoic and Cenozoic sedimentary successions that
 196 cover much of the Arabian Peninsula.

197 The Mesopotamian Foredeep extends from southeastern Turkey through Iraq toward the Persian
 198 Gulf, forming a major sedimentary basin filled with thick Cenozoic deposits. This basin developed in
 199 response to the collision between the Arabian and Eurasian plates, which also produced the highly
 200 deformed Zagros Fold-and-Thrust Belt along the northeastern margin of the Arabian Plate. Similar
 201 tectonic deformation characterizes the Bitlis Suture Zone in southeastern Turkey. To the west, the Dead
 202 Sea Fault System marks a major transform boundary extending from the Gulf of Aqaba northward through
 203 the Levant. Further south, the Red Sea and Gulf of Aden represent young rift systems associated with the
 204 separation of Arabia from Africa. These regions are characterized by extensive Cenozoic volcanic rocks
 205 and active faulting. The East African Rift continues southward from the Gulf of Aden, linking Middle
 206 Eastern tectonics with those of eastern Africa. Overall, the region records the interaction of ancient
 207 continental crust, extensive sedimentary basins, active rifting, transform faulting, and continental collision
 208 (Sembroni et al., 2024).
 209



210
 211

212 **Figure 3.** Geological map of the study area. Modified from Sembroni et al. (2024). The Arabian-Nubian Precambrian Shield is
213 highlighted by a dashed red line.

214

215 *2.3. Paleogeographical and tectonic evolution*

216

217 The dynamics of the Arabian Plate and its precursor over time have been crucial for mangrove
218 biogeography, not only in the study area but also on a global scale, particularly with respect to the
219 westward biotic interchange between the IWP region and present-day Europe (Rull, 2026).

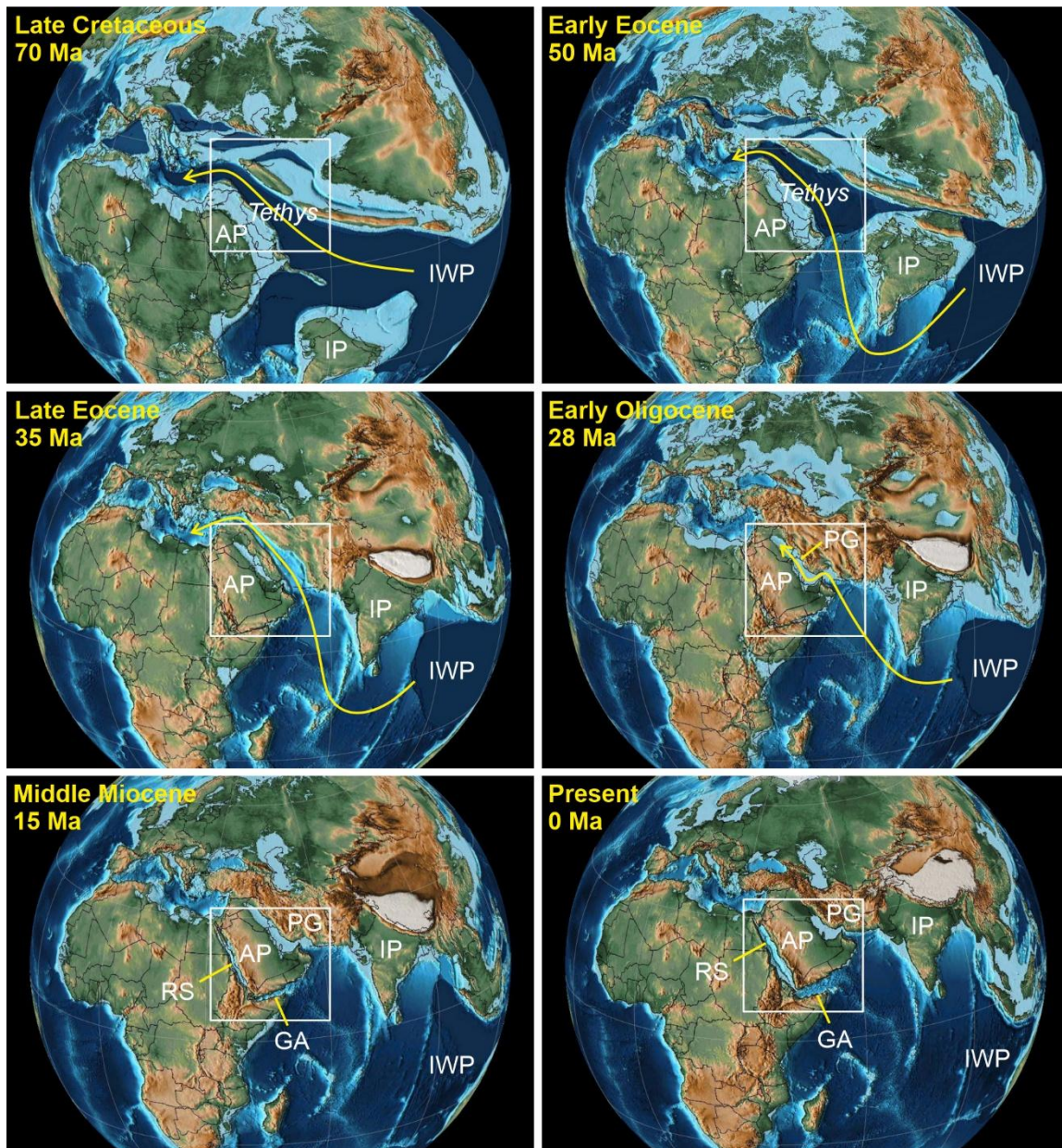
220 During the Late Cretaceous (ca. 70 Ma), the area now occupied by the Arabian Plate was part of
221 the African Plate complex, specifically the Nubian Plate, which migrated northeastward and was
222 separated from the Eurasian Plate by the Tethys Sea (Fig. 4). At that time, the Indian Plate, in its northward
223 migration, had not yet reached low latitudes, and a continuous Tethyan corridor facilitated east–west
224 dispersal and migration of tropical biota. The Arabian Plate had not yet separated from the Nubian Plate
225 (Fig. 2) and formed part of its northeastern margin, a typical Mesozoic configuration (Giraud & Bosworth,
226 1999). In the Early Eocene (50 Ma), the Tethyan connection still existed, but the Indian Plate had reached
227 the Eurasian Plate, and the available marine pathway for IWP biota to disperse westward had to adopt a
228 more southerly route to bypass the Indian wedge. A similar configuration persisted during the Late Eocene
229 (35 Ma), although the marine connection had become considerably shallower due to the progressive
230 convergence of the African and Eurasian plates.

231 The closure of the Tethys seaway occurred during the Oligo–Miocene transition, with estimates
232 ranging from 27 to 21 Ma (Pirouz et al., 2017; Torfstein & Steinberg, 2020). This event broadly coincided
233 with the break-up of the Arabian Plate from the Nubian Plate, which began in the Late Oligocene (~25 Ma)
234 (Stern & Johnson, 2010). Further independent rifting of the Arabian Plate as an isolated plate led to the
235 opening of the Red Sea through separation from the Nubian Plate at approximately 25 Ma (Bosworth et
236 al., 2005; Bosworth, 2015), and of the Gulf of Aden through separation from the Somali Plate at
237 approximately 20 Ma (Fournier et al., 2010). Present-like configuration was established by the Middle
238 Miocene (~15 Ma), except for the continued opening of the Red Sea and the Gulf of Aden, as well as
239 ongoing shortening and deepening of the Arabian Gulf, whose modern shoreline was attained only very
240 recently following the last glaciation (Lambeck, 1996).

241 The collision of the Arabian and Eurasian plates produced the Zagros Range as a major collisional
242 fold–thrust belt (Sembroni et al., 2024) (Fig. 2). According to Alavi (2007), continued convergence
243 shortened and thickened the former Arabian passive margin through a combination of basement-involved
244 thrusting and detachment folding within the sedimentary cover, generating the elongated anticlines and
245 thrust systems that characterize the Zagros today. The growing orogenic load simultaneously flexed the
246 Arabian lithosphere downward, creating the Mesopotamian–Persian Gulf foreland basin, also known as
247 the Zagros foreland basin. This subsiding basin acted as a major depocenter for sediments eroded from
248 the uplifting Zagros range, linking tectonic deformation, mountain building, and foreland sedimentation
249 within a coupled tectono-sedimentary system.

250 In the easternmost sector of the Arabian Plate, presently northeastern Oman, oceanic lithosphere
251 of the Arabian Sea began to subduct northward beneath the Eurasian margin following the Tethys closure,
252 forming the Makran subduction zone and the Oman foreland basin, behind the Oman Range. This process
253 generated an active accretionary prism and forearc basin system along the margin of the Gulf of Oman,
254 characterized by sediment accretion, thrust imbrication, and progressive outward growth of the
255 submarine wedge (Kopp et al., 2000).

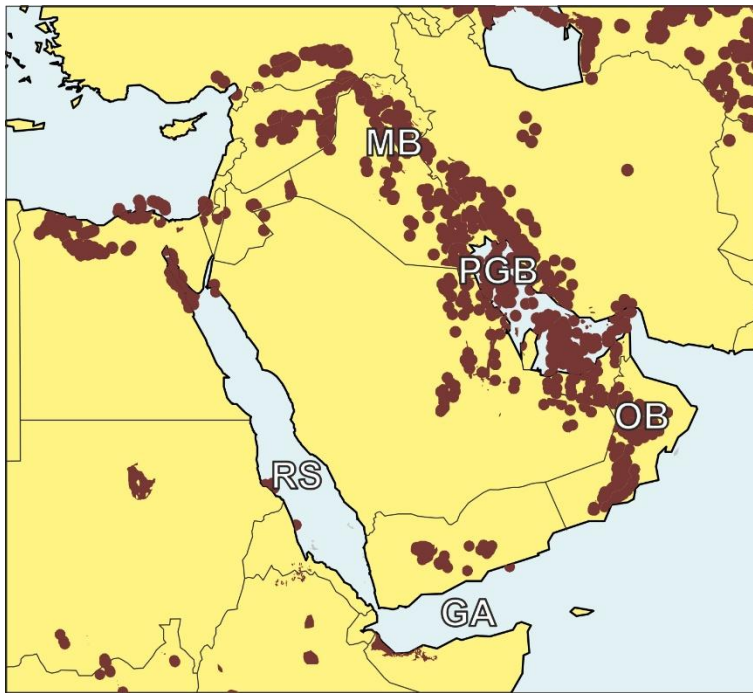
256



257
 258
 259 **Figure 4.** Late Cretaceous to present global paleogeographical trends taking the present Middle East position as the reference
 260 (white box). Time slices were selected according to the main paleogeographical shifts potentially significant for mangrove
 261 dynamics in the study area and its eventual influence on regional patterns. Maps were generated with GPlates 2.5.0 using the
 262 Scotese (2016) PALEOMAP PaleoAtlas, freely available at <https://www.earthbyte.org/paleomap-paleoatlas-for-gplates/> (last
 263 accessed May 21, 2026). AP, Arabian Plate or its precursor; IP, Indian Plate; GA, Gulf of Aden; PG, Persian Gulf; RS, Red Sea.

264
 265 **2.4. Petroleum geology**

266
 267 The stratigraphic interval spanning the Late Cretaceous, Paleogene and Neogene – which is the focus of
 268 this review – constitutes the primary reservoir-seal architecture responsible for the world's largest
 269 hydrocarbon accumulations in the ME. The main oil/gas fields are concentrated along the Africa/Eurasia
 270 collision zone, in the Mesopotamian, Persian Gulf and Oman foreland basins (Fig. 5). This distribution is
 271 relevant for understanding the geographic pattern of fossil localities in the MESMA dataset, as discussed
 272 in Section 3.3. The formation of the ME petroleum system, which is largely linked to the tectonic evolution,
 273 was compiled by Alsharan & Nairn (1997), and can be summarized as follows.
 274



275
276
277
278
279
280
281

Figure 5. Oil/gas fields (brown) in the study area. Note the main concentration along the collision zone of the Mesopotamian (MB), Persian Gulf (PGB) and the Oman (OB) foreland basins, in contrast to the rifting zones of the Red Sea (RS) and the Gulf of Aden (GA) basins. Downloaded and modified from the U.S. National Energy Technology Laboratory (<https://arcgis.netl.doe.gov>; last accessed May 16, 2026).

282
283
284
285
286
287
288
289
290

During the Late Cretaceous, a prolonged period of high sea levels and stable subsidence across the Arabian Plate facilitated the development of extensive, high-productivity carbonate platforms characterized by shallow-marine limestones that exhibit excellent primary porosity and substantial lateral continuity, functioning as the region's most prolific regional reservoir rocks. This dominant carbonate regime persisted into the Paleogene within the Tethys shallow-marine domain, but subsequent tectonic compression related to the early phases of the Zagros orogeny induced widespread natural fracturing within these Cenozoic limestone successions, a structural overprint that significantly enhanced secondary permeability and transformed these otherwise dense carbonates into highly efficient, high-flow-rate reservoirs.

291
292
293
294
295
296
297
298
299

The entire petroleum system was finalized and structurally sealed during the Neogene due to the definitive collision between the Arabian and Eurasian plates, a major tectonic event that compressed the thick sedimentary package into high-amplitude, continuous anticlinal folds to create massive structural traps, while concurrently restricting the marine basin to induce hyper-saline conditions that deposited thick, regionally extensive evaporite sequences, primarily composed of halite and anhydrite, which now provide an absolute top seal that prevents vertical hydrocarbon migration and ensures the long-term preservation of the immense underlying Paleogene and Cretaceous oil accumulations.

299 *2.2. Extant mangroves and climatic insights*

300
301
302
303
304
305
306
307
308
309
310

Most extant mangroves are located along the coasts of the Red Sea and the Persian Gulf (also known as the Arabian Gulf), with fewer occurrences in the Gulfs of Aden and Oman and only scattered occurrences in the Arabian Sea. The northernmost ME mangrove (Wadi Kid; $\sim 28^{\circ}10'N$) is located on the southern Sinai Peninsula (Fig. 2) and is also the northernmost mangrove in the entire IWP region (Por et al., 1977).

Mangrove extent is very limited, with a total area of $\sim 320 \text{ km}^2$, reaching maxima in Iran ($\sim 75 \text{ km}^2$) and in Eritrea and the United Arab Emirates ($70 \sim \text{km}^2$ each), and minima ($< 2 \text{ km}^2$) in Egypt, Oman and Bahrain (raw data from Bunting et al., 2020). These figures are very low compared with those of other regions of similar extent, such as the Caribbean coasts, which has a total mangrove area of approximately $14,700 \text{ km}^2$, or southeast Asia, with $48,200 \text{ km}^2$ (Bunting et al., 2022; Rull, 2024). In general, climatic conditions in the ME are unfavorable for mangrove development (Quistoudt et al., 2012), with average

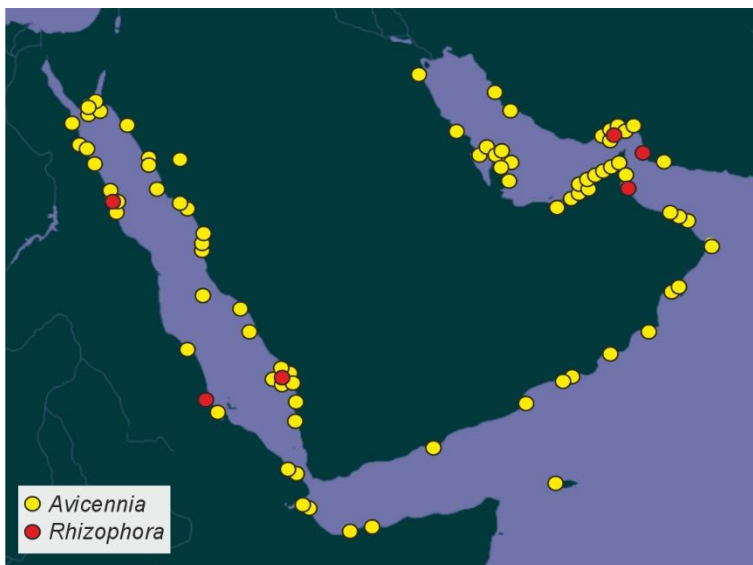
311 temperatures ranging from about 20 °C in the northwest to 30 °C in the southeastern Arabian Peninsula
 312 (and seawater temperatures reaching up to 28 °C in summer), along with very low precipitation (generally
 313 less than 100 mm per year on average, with maxima around 250 mm) (Patlakas et al., 2019; Waleed et al.,
 314 2025). In addition, the absence of large, permanent freshwater inputs significantly reduces the supply of
 315 coastal sediments and nutrients required for mangrove growth and promotes hypersaline conditions
 316 (exceeding 40 ppt) in adjacent seas, beyond the tolerance range of most mangrove species (Waleed et al.,
 317 2025).

318 Under these conditions, only two highly tolerant true-mangrove species—out of more than 50
 319 recorded in the IWP region (Table 1)—are able to persist: *Avicennia marina* and *Rhizophora mucronata*
 320 (Waleed et al., 2025). Saenger et al. (2019) mention the scattered occurrence of *Bruguiera* and *Ceriops*
 321 but do not provide the original references supporting these records. A search of the Global Biodiversity
 322 Information Facility (GBIF; <https://www.gbif.org/>; last accessed on 13 May 2026) did not retrieve any
 323 occurrence records of these genera from the ME region. Furthermore, detailed studies of the region (e.g.,
 324 Haseeba et al., 2025a, b; Waleed et al., 2025) do not report the occurrence of either genus.

325 *A. marina* occurs throughout ME mangroves and consistently dominates the canopy, whereas *R.*
 326 *mucronata* is rare or absent, being restricted to localized settings with some freshwater input from
 327 streams, which are uncommon in the region (Haseeba et al., 2025a, b; Waleed et al., 2025) (Fig. 6). Both
 328 species display a range of morphological, physiological, reproductive and phenological adaptations that
 329 enable them to cope with these harsh conditions. Nevertheless, stress from high temperatures, aridity,
 330 and limited sediment and nutrient availability constrains growth, resulting in dwarf forms of *A. marina*
 331 and *R. mucronata* compared with populations of the same species elsewhere in the IWP region (Waleed
 332 et al., 2025). This situation contrasts with other IWP mangroves located within the same latitudinal range
 333 but under more favorable environmental conditions, which are among the healthiest and most diverse in
 334 the pantropical belt (Tomlinson, 2016; Duke, 2017). This makes ME a biogeographically distinct mangrove
 335 province within the IWP region, differing from other provinces such as East Africa, South Asia, Southeast
 336 Asia and East Asia–Australasia (Saenger et al., 2019).

337 Mangrove research has experienced an exponential increase during the 21st century, particularly
 338 along the Persian Gulf and Red Sea coasts of Iran, Saudi Arabia, and Egypt, where these ecosystems are
 339 most extensively distributed (Fig. 2). The predominant research themes focus on human-related issues,
 340 including baseline ecological characterization, environmental impacts, management, and conservation.
 341 Concerns about the future of Middle Eastern mangroves under ongoing global change have become a
 342 major driver of research in the region (Friis & Burt, 2020).

343



344

345

346 **Figure 6.** Comparison between *Avicennia* and *Rhizophora* occurrences in the Middle East mangroves according to the Global
 347 Biodiversity Information Facility (GBIF; <https://www.gbif.org/>; last accessed, 13 May 2026).

348

349

350 3. The MESMA dataset

351 352 3.1. Methodological hints

353
354 This synthesis is based on the MESMA (Middle East MAngroves) dataset, which gathers the published
355 studies, preferably original sources whenever possible; review papers are not used as primary sources of
356 evidence. In a region with as much oil activity as the ME, many studies are never made public because the
357 information is considered confidential by the various operating companies. This means that it is difficult
358 to determine whether an area or a time interval with little available information is genuinely understudied
359 or simply subject to a higher level of confidentiality. Therefore, gaps in information are difficult to
360 interpret and cannot a priori be considered evidence of absence. Since the subject of study—mangroves—
361 are coastal ecosystems, it is expected that their fossils will be found preferentially in transitional land-sea
362 sedimentary environments and will be scarcer or absent in more continental or marine settings.
363 Consequently, lithology and sedimentology may provide useful information for interpreting possible
364 information gaps.

365 Searches were conducted within the available global literature syntheses mentioned above, as
366 well as in standard bibliographic databases, mainly Web of Science, Scopus, Google Scholar, OpenAlex,
367 The Lens and BASE, along with the large and comprehensive fossil pollen database PALYNODATA (White,
368 2008). The search criteria consisted of combinations of geographical names (countries, seas, gulfs),
369 chronostratigraphic units (periods, epochs, ages) and extant/fossil taxonomic terms from Table 1. Reviews
370 and syntheses were also used to identify the original references in which the primary evidence was
371 published, and the most recent papers were examined to locate older literature. When geographical
372 coordinates were not provided in the original references, the locality was determined using Google Earth.
373 In a few cases (e.g., Lake Nasser), the exact locality is not provided, and the point on the map is placed
374 approximately at the center of the study area. The data were not reinterpreted, and the original
375 information on age, location and taxonomy was reported.

376 The fossils considered include pollen and macroremains (e.g., roots, wood, leaves, fruits), or their
377 corresponding impressions or molds, from vascular plants whose nearest living relatives (NLRs) belong to
378 the genera listed in Table 1 as major and minor true-mangrove elements and their associated taxa. In
379 some cases, fossils were identified in the original literature by their NLRs (e.g., *Avicennia*), whereas in
380 others the form genus was used (e.g., *Spinizonocolpites* for *Nypa*). In this review, the NLR names are used
381 for consistency. When available, descriptions and images provided in the original references were used
382 to verify taxonomical identity and botanical affinities.

383 A conservative evidence-based approach was adopted, and only fossils reliably attributed to
384 known mangrove taxa, as listed in Table 1, were used. Mangroves are regarded as ecosystems, rather
385 than as sedimentary environments. Indeed, they are not merely coastal or intertidal ecosystems adapted
386 to flooding and salinity, but rather well-defined and characteristic taxonomic, physiognomic, structural,
387 biogeographical and ecological communities (Chapman, 1976; Saenger, 2003; Tomlinson, 2016). Other
388 coastal communities—e.g., beach forests, swamp forests, salt marshes or seagrass meadows—may also
389 be adapted to intertidal environments and variable salinity without constituting mangroves. For this
390 reason, inferences regarding the presence of mangrove communities based solely on sedimentological
391 reconstructions of coastal or tidal environments, without taxonomic and ecological support, were not
392 considered.

393 The use of fossil taxa with unclear botanical affinities that are associated in the literature with
394 “mangrove” or “mangrove-like” vegetation/environments for non-biological reasons was also avoided.
395 This includes, for example, fossil remains of extinct plants whose mangrove affinity is inferred rather than
396 demonstrated, as in the case of the fern fossil *Weichselia* (Smith et al., 2001). This example is discussed in
397 more detail in the paleobiogeography section (4.1). Unidentified remains or ichnofossils attributed to
398 mangrove vegetation were likewise excluded from the analysis—although they are mentioned in the
399 location list for completeness (Table 2)—to avoid ambiguous interpretations. For example, fossil rod-like
400 structures interpreted as mangrove roots (pneumatophores) are seldom preserved, although some have
401 later been reinterpreted as trace fossils (burrows) produced by marine invertebrates, or as composites of
402 pneumatophores and burrows produced by unknown organisms (Gee et al., 2019; Abdel-Fattah &

403 Gingras, 2020). A paper reporting particulate organic matter presumed to be of mangrove origin (Hamzeh
 404 et al., 2025) is also listed for completeness but not used in the biogeographical analysis. The same applies
 405 to features such as “mangrove peat” or “mangrove (paleo)soil” (e.g., Kenig et al., 1989).

406 Faunal fossils and remains linked to mangrove ecosystems through modern analogs, such as
 407 mollusks and foraminifera (e.g., Ghandour et al., 2021; Hamzeh et al., 2025), are not included in the
 408 analysis. This is not intended to dismiss such relationships, which are ecologically consistent in modern
 409 settings, but rather reflects the fact that this review is limited to plant fossils as representatives of the
 410 fundamental taxonomic and structural basis of these ecosystems. In any case, studies of mangrove-
 411 related fossil fauna constitute only a small portion of the retrieved ME literature.

412 These criteria favor evidence-based evolutionary and biogeographical reconstructions and reduce
 413 reliance on speculative interpretations. They also minimize the risk of circular reasoning and the
 414 propagation of misinterpretations in the literature. It is both easier and more scientifically sound to add
 415 a new mangrove component to the database once its affinity with this ecosystem has been demonstrated
 416 than to correct the database—and the associated misinterpretations—if the taxon is later shown not to
 417 belong to mangrove ecosystems.

418 The chronostratigraphical framework of this study was provided by latest version of the
 419 International Chronostratigraphic Chart (Cohen et al., 2013; v. 2024-12). Epochs and age boundaries are
 420 indicated using a slash (e.g., Paleocene/Eocene), whereas age ranges are expressed with a dash (e.g.,
 421 Middle-Late Miocene). Global paleotemperature and paleoeustatic trends were taken from Westerhold
 422 et al. (2020) and Miller et al. (2020), respectively.

423

424 3.2. General observations

425

426 The MESMA dataset is presented in Table 2 and Fig. 7. It includes 78 localities distributed across 12
 427 countries, with Egypt being the most represented (20%), followed by Turkey (18%), Sudan (15%) and
 428 Oman (13%). The least represented countries (1% or less) are Iran, Iraq, Ethiopia and Qatar. Saudi Arabia,
 429 Somalia, UAE and Yemen occupy intermediate positions (3-8%). No records were found for Bahrain,
 430 Djibouti, Eritrea, Israel, Jordan, Kuwait, Lebanon, Palestine or Syria.

431 Geologically, 31% of the records are Cretaceous, 29% Paleogene, 17% Neogene, and 22%
 432 Quaternary. Cretaceous records are concentrated mainly in northeastern Africa, whereas Paleogene and
 433 Neogene sites are predominantly located in Egypt and Turkey, and Quaternary localities are more
 434 frequent on the southeastern Arabian Peninsula. Taxonomically, only five of the 20 known true mangrove
 435 genera (Table 1) are represented. Three of these genera (*Avicennia*, *Nypa* and *Rhizophora*) are mangrove-
 436 forming trees, whereas the other two (*Acrostichum* and *Pelliciera*) are minor mangrove components.
 437 Three genera (*Acrostichum*, *Avicennia* and *Rhizophora*) are globally distributed in modern mangroves,
 438 whereas the other two are restricted either to the Indo-West Pacific (IWP) region (*Nypa*) or the Atlantic-
 439 East Pacific (AEP) region (*Pelliciera*). The case of *Pelliciera* is particularly noteworthy because it is
 440 considered a genuine AEP element, and its occurrence in Cenozoic records from Europe and the Middle
 441 East has been questioned following detailed morphological analyses of fossil pollen (Rull, 2025). As in the
 442 European dataset (EURMA), *Pelliciera* records are included in this analysis to preserve the original
 443 evidence, although their reliability is considered in the interpretations (Rull, 2026).

444

445 3.3. Geographical patterns

446

447 Some regions are more extensively represented than others in the MESMA dataset (Fig. 7). The areas with
 448 the highest number of mangrove records are the Anatolian Peninsula, northeastern Africa, especially
 449 Egypt, and the southeastern Arabian Peninsula, notably Oman and the UAE. Less represented areas
 450 include the interior Arabian Peninsula, the Levant, and southwestern Asia, especially Iran and Iraq. Based
 451 on the available evidence, it remains difficult to determine to what extent this pattern reflects
 452 chronostratigraphical or paleoenvironmental constraints, differential preservation, research bias,
 453 confidentiality practices of oil companies or cultural differences.

454 Geological constraints occur in areas where exposed rocks are older than the Late Cretaceous—
 455 when the first mangrove records appeared globally—or where sedimentary environments were

456 unsuitable for mangrove growth and/or preservation, notably in inland and open/deep-marine settings.
457 In the study area, the absence of prospective rocks for chronostratigraphic reasons is largely restricted to
458 the Precambrian Arabian–Nubian Shield, whereas Late Cretaceous and Cenozoic sediments are widely
459 distributed across the remaining regions (Fig. 3). The lack of suitable sedimentary environments occurs
460 mainly in the Red Sea (RS) and Gulf of Aden (GA) basins, which are largely devoid of Cenozoic terrestrial
461 fossils in general.

462 Indeed, as rifting basins, the RS and GA sediments consist mainly of marine and marginal-marine
463 siliciclastics, evaporites, and carbonates, reflecting progressively increasing water depths that culminated
464 in foram-rich marls and deep-water limestones by the Early Miocene (Hughes & Johnson, 2005). Between
465 the Early and early Middle Miocene, coinciding with the Arabia–Eurasia collision, sedimentation shifted
466 to marine mudstones and submarine evaporites, although deep-water environments persisted. The
467 development of extensive carbonate platforms was typical of this interval (Koeshidayatullah et al., 2015).
468 The Middle Miocene was characterized by continued oceanic spreading and the deposition of thick
469 evaporites, followed in the Late Miocene by shales and anhydrites. Finally, during the Pliocene and
470 Pleistocene, sedimentation became predominantly alluvial, with coarse sands and gravels prevailing. In
471 summary, marine and deep-marine environments—rather than the coastal intertidal settings required for
472 mangrove development—dominated throughout the time interval considered in this study.

473 Some pollen occurrences are reported in review and summary papers about RS and GA regions,
474 although the localities and ages are not specified with the precision required for this study. For example,
475 Filatoff & Hughes (1996) noted the occurrence of pre-rifting (Late Cretaceous–Early Paleogene) palm and
476 fern floras typical of tropical humid climates, followed by syn-rift assemblages dominated by savanna-
477 type grass vegetation and Neogene halophytic plants characteristic of arid sabkha environments. The only
478 mention of mangroves concerns Cretaceous–Paleocene *Nypa*, previously reported by Srivastava & Binda
479 (1991), as well as sporadic occurrences of Miocene *Avicennia*-type pollen, although no further details are
480 provided. The same authors also noted that other mangrove elements common in tropical regions
481 elsewhere, such as *Rhizophora* or *Sonneratia*, are rare in the fossil record. Hughes & Johnson (2005)
482 likewise mentioned some pollen occurrences but without reference to mangroves. A few more detailed
483 Paleogene–Neogene studies are available and are included in this synthesis (Table 2; Fig. 7), with the
484 exception of Moltzer & Binda (1981, 1984), which did not report mangrove pollen.

485 The situation in the RS–GA region contrasts with that of the Mesopotamian–Persian Gulf and
486 Oman basins, where Cenozoic rocks are abundant and have been fundamental to the development of
487 petroleum systems, as noted above. Therefore, neither geological constraints nor a lack of economic
488 interest can be invoked to explain the scarcity of mangrove records in the MESMA dataset. In this case,
489 confidentiality issues are likely involved. As a former exploration biostratigrapher at a major Caribbean oil
490 company (Rull, 2002), the author is aware of the large volume of biostratigraphic information contained
491 in internal company reports, or not reported at all, that remains unavailable for reviews and syntheses
492 such as the present study. Based on the available evidence, it is not possible to assess the significance of
493 this situation for the ME region. Interestingly, however, most records from the Persian Gulf and the Gulf
494 of Oman correspond to the Holocene, which is of less interest to the oil industry. The lack of mangrove
495 records across extensive continental areas of southwestern Asia—including Syria, Iran, Iraq, and the
496 Levant—is striking and, based on the available evidence, remains difficult to explain.

497 Cultural differences among countries, reflected in variable research effort and publication
498 intensity, may also contribute to the observed geographical patterns in evidence availability. For example,
499 Egypt has a more established tradition of publishing palynostratigraphic data than other countries in the
500 region with comparable levels of oil-industry activity. A similar situation exists in Turkey, where
501 biostratigraphic research has been closely linked to the coal industry, as the country ranks among the
502 world's major lignite producers (Yilmaz, 2006). Despite their strategic importance as energy producers,
503 both countries have a long tradition of stratigraphic research and fossil documentation, including records
504 of terrestrial vegetation and mangrove ecosystems.

505
506
507**Table 2.** The MESMA dataset. Fossil localities compiled in this review and their main features (see Fig. 7 for location). Fossil types: CH, charcoal; FS, fruits/seeds; LF, leave molds/impressions; PO, particulate organic matter; PS, pollen/spores; PT, peat; RT, roots casts/molds/rhizoliths; RZ, rhizomes; SL, soils/paleosols; TS, trunks/twigs/stems; WF, wood fragments.

Map	Site	Country	Latitude	Longitude	Period	Epoch	Age	Mangrove taxa	Fossil type	References
Qm	Qeshm	Iran	26°51'08"N	55°39'49"E	Quaternary	Holocene	L Holocene	Unidentified	PO	Hamzeh et al. (2020)
Fi	Filim	Oman	20°36'36"N	58°10'12"E	Quaternary	Holocene	M-L Holocene	<i>Rhizophora</i> <i>Avicennia</i>	PS	Lézine et al. (2017)
KJ	Kwar-al-Jaramah	Oman	22°29'24"N	59°45'36"E	Quaternary	Holocene	M-L Holocene	<i>Rhizophora</i> <i>Avicennia</i>	PS	Lézine (2009) Lézine et al. (2017)
Sy	Suwayh	Oman	22°05'35"N	59°40'01"E	Quaternary	Holocene	M-L Holocene	<i>Rhizophora</i> <i>Avicennia</i>	PS CH	Lézine et al. (2002, 2010) Berger et al. (2013)
AD	Abu Dhabi	Oman	24°27'00"N	54°26'24"E	Quaternary	Holocene	M-L Holocene	Unidentified	RT	Khanna et al. (2021)
RR	Ras ar Ru'ays	Oman	22°10'54"N	59°45'47"E	Quaternary	Holocene	M Holocene	<i>Avicennia?</i>	RT	Decker et al. (2020)
Al	Alashkara	Oman			Quaternary	Holocene	M Holocene	<i>Avicennia</i>	WF RT	Berger et al. (2013)
Qy	Quriyat	Oman	23°15'47"N	58°54'57"E	Quaternary	Holocene	M Holocene	<i>Avicennia?</i>	RT	Decker et al. (2020)
Sw	Sawadi	Oman	23°35'16"N	58°22'58"E	Quaternary	Holocene	M Holocene	<i>Avicennia?</i>	RT	Decker et al. (2020)
AD	Abu Dhabi	UAE	24°17'47"N	54°20'35"E	Quaternary	Holocene	Holocene	Unidentified	PT/SL/RT/TS	Kenig et al. (1989)
Mi	Sabkha Matti	UAE	23°50'36"N	52°01'50"E	Quaternary	Pleistocene Holocene	Pleistocene Holocene	Unidentified	RT	Kirkham (1998)
92	MD92-1002	Yemen	12°01'32"N	44°19'02"E	Quaternary	Holocene	E-M Holocene	<i>Rhizophora</i> <i>Avicennia</i>	PS	Fersi et al. (2016)
76	MD 76 135	Yemen	14°26'06"N	50°31'03"E	Quaternary	Pleistocene Holocene	L Pleistocene Holocene	<i>Avicennia</i> <i>Rhizophora</i>	PS	Van Campo et al. (1982)
Z1	Zeugen 1	UAE	24°05'47"N	53°42'48"E	Quaternary	Pleistocene	L Pleistocene	Unidentified	RT	Wood et al. (2012)
Z4	Zeugen 3-4	UAE	24°19'15"N	54°15'07"E	Quaternary	Pleistocene	L Pleistocene	Unidentified	RT	Wood et al. (2012)
Z5	Zeugen 5	UAE	25°11'49"N	55°19'04"E	Quaternary	Pleistocene	L Pleistocene	Unidentified	RT	Wood et al. (2012)
23	DSDP 231	Somalia	11°53'24"N	48°15'00"E	Neogene Quaternary	Miocene Pleistocene	Tortonian M Pleistocene	<i>Rhizophora</i>	PS	Bonnefille (2010)
GH	GH 404-2A	Egypt	27°46'36"N	33°46'21"E	Neogene	Miocene	Burdigalian Langhian	<i>Rhizophora</i>	PS	El Atfy et al. (2017)
Kt	Kultak	Turkey	37°04'42"N	27°56'24"E	Neogene	Miocene	L Burdigalian Langhian	<i>Avicennia</i> <i>Acrostichum</i>	PS	Kayseri-Özer (2014)
Dm	Dawmat	Saudi Arabia	27°33'37"N	48°37'53"E	Neogene	Miocene	E-M Miocene	<i>Avicennia?</i>	RT	Whybrow & McClure (1980/81)
Br	Barakah	UAE	24°04'14"N	52°26'17"E	Neogene	Miocene	E-M Miocene	<i>Avicennia?</i>	RT	Whybrow & McClure (1980/81)
EM	El Mellaha	Egypt	27°13'17"N	33°47'36"E	Neogene	Miocene	Aquitanian Burdigalian	<i>Nypa</i> ¹	PS	El Diasty et al. (2020)
Dz	Denizli	Turkey	37°46'59"N	29°05'47"E	Neogene	Miocene	Aquitanian	<i>Acrostichum</i>	PS	Kayseri-Özer (2014)
Ke	Kale	Turkey	37°27'05"N	28°48'47"E	Neogene	Miocene	Aquitanian	<i>Acrostichum</i>	PS	Kayseri-Özer (2014)

This is a non-peer-reviewed preprint submitted to EarthArXiv

Tv	Tavas	Turkey	37°34'23"N	29°04'17"E	Neogene	Miocene	Aquitania	<i>Acrostichum</i>	PS	Kayseri-Özer (2014)
Bd	Burdur	Turkey	37°43'06"N	30°16'56"E	Neogene	Miocene	Aquitania	<i>Acrostichum</i>	PS	Kayseri-Özer (2014)
A2	Melut AY2	Sudan	10°34'37"N	33°05'56"E	Neogene	Miocene	E Miocene	<i>Rhizophora</i>	PS	Eisawi (2007)
A3	Melut AY3	Sudan	09°45'33"N	33°11'44"E	Neogene	Miocene	E Miocene	<i>Rhizophora</i>	PS	Eisawi (2007)
AG	Abu Gharadig	Egypt	29°43'45"N	28°32'18"E	Neogene	Miocene	E Miocene	<i>Acrostichum</i>	PS	Ibrahim et al. (2024)
HS	Hilal-Shoab Ali	Egypt	27°46'36"N	33°46'21"E	Neogene Paleogene	Oligocene Miocene	Chattian Aquitania	<i>Rhizophora</i>	PS	El Atfy et al. (2013)
Aa	Amana-1X	Egypt	29°33'24"N	29°25'24"E	Paleogene	Oligocene	Oligocene E Miocene	<i>Rhizophora</i> <i>Pelliciera</i> ²	PS	El Atfy et al. (2022)
Cg Mr	Chilga Margargaria	Ethiopia	12°30'35"N 12°30'31"N	36°52'05"E 37°06'57"E	Paleogene	Oligocene	L Oligocene	<i>Acrostichum</i>	LF	Jacobs et al. (2005) García Massini et al. (2006, 2010) Pan et al. (2006)
Ma	Mugla	Turkey	37°12'55"N	28°21'48"E	Paleogene	Oligocene	Rupelian	<i>Acrostichum</i> <i>Avicennia</i> <i>Pelliciera</i> ²	PS	Kayseri-Özer (2014)
Ms	Milas	Turkey	37°18'42"N	27°46'51"E	Paleogene	Oligocene	Rupelian	<i>Acrostichum</i> <i>Avicennia</i> <i>Pelliciera</i> ²	PS	Kayseri-Özer (2014)
Me	Mersin	Turkey	36°38'43"N	34°38'29"E	Paleogene	Oligocene	Rupelian	<i>Nypa</i>	PS	Kayseri-Özer (2014)
Mu	Mut	Turkey	36°38'43"N	33°26'13"E	Paleogene	Oligocene	Rupelian	<i>Nypa</i>	PS	Kayseri-Özer (2014)
Qt	Qattara	Egypt	29°40'53"N	27°07'09"E	Paleogene	Eocene Oligocene	L Eocene E Oligocene	<i>Pelliciera</i> ²	PS	El Atfy et al. (2021)
Dk	Duhok	Iraq	36°52'00"N	43°03'40"E	Paleogene	Eocene	M-L Eocene	<i>Nypa</i> <i>Pelliciera</i> ²	PS	Al-Atrushe & Al-Hasson (2025)
Ht	Wadi Al-Hitan	Egypt	29°16'15"N	30°01'26"E	Paleogene	Eocene	Bartonian Priabonian	<i>Nypa</i> ? <i>Avicennia</i> ? <i>Rhizophora</i> ?	RZ/RT	El-Saadawi (2005) El-Saadawi et al. (2018)
AK	Al-Khor	Qatar	25°40'49.47"N	51°29'48.66"E	Paleogene	Eocene	Lutetian Bartonian	Unidentified	TS?	Sadooni & Al-Saad (2012)
Mk	Mokattam	Egypt	30°01'18"N	31°18'12"E	Paleogene	Eocene	Lutetian	<i>Nypa</i>	FS	Fraas (1867) Bonnet (1904) Kräusel & Stromer (1924) Kräusel (1939) Chandler (1954)
Kw	Al Khawd	Oman	23°33'57"N	58°07'25"E	Paleogene	Eocene	Lutetian	<i>Nypa</i>	PS	Racey et al. (2025)
Sv	Sivrihisar	Turkey	39°27'05"N	31°32'16"E	Paleogene	Eocene	Ypresian Lutetian	<i>Nypa</i>	PS	Akkiraz et al. (2022)
Yg	Yozgat	Turkey	39°49'16"N	34°48'31"E	Paleogene	Eocene	M-L Eocene	<i>Avicennia</i> <i>Pelliciera</i> ² <i>Nypa</i>	PS	Akkiraz et al. (2008)
Sg	Sorgun	Turkey	39°48'46"N	35°11'25"E	Paleogene	Eocene	M-L Eocene	<i>Avicennia</i>	PS	Akkiraz et al. (2008)

This is a non-peer-reviewed preprint submitted to EarthArXiv

									<i>Pelliciera</i> ²	
									<i>Nypa</i>	
Jd	Jeddah	Saudi Arabia	21°31'45"N	39°09'40"E	Paleogene	Eocene	Ypresian	<i>Nypa</i>	PS	Srivastava & Binda (1991)
As	Aswan	Egypt	23°39'08"N	32°11'27"E	Paleogene	Eocene	E Eocene	<i>Nypa</i>	FS	El-Noamani & Ziada (2025)
Kw	Al Khawd	Oman	23°33'57"N	58°07'25"E	Paleogene	Eocene	E Eocene	<i>Nypa</i>	PS	El Beialy (1998)
									<i>Avicennia</i>	
Dz	Denizli	Turkey	37°46'59"N	29°05'47"E	Paleogene	Eocene	Eocene	<i>Acrostichum</i>	PS	Kayseri-Özer (2014)
									<i>Pelliciera</i> ²	
									<i>Nypa</i>	
Am	Armutalani	Turkey	37°53'47"N	29°36'13"E	Paleogene	Eocene	Eocene	<i>Acrostichum</i>	PS	Kayseri-Özer (2014)
									<i>Pelliciera</i> ²	
									<i>Nypa</i>	
Qs	Quseer/Kosseir	Egypt	26°05'05"N	34°16'49"E	Paleogene	Paleocene	Danian	<i>Nypa</i>	FS	Chandler (1954)
Ns	Lake Nasser	Egypt	22°42'22"N*	32°11'50"E*	Paleogene	Paleocene	ND	<i>Nypa</i>	FS	Lejal-Nicol (1987)
Mq	Abu Minqar	Egypt	26°31'05"N	27°39'43"E	Cretaceous	Cretaceous	Maastrichtian	<i>Nypa</i> ³	FS	Gregor & Hagn (1982)
					Paleogene	Paleocene	Danian		PS	Tantawy et al. (2001)
										El-Soughier et al. (2011)
										El Soughier (2020)
										Abu El-Kheir et al. (2021)
										El-Hedeny et al. (2021)
Kk	Kaikang	Sudan	09°21'00"N	29°07'37"E	Cretaceous	L Cretaceous	L Maastrichtian	<i>Nypa</i>	PS	Cole et al. (2017)
Ko	Kosti	Sudan	13°07'59"N	32°38'28"E	Cretaceous	L Cretaceous	Maastrichtian	<i>Nypa</i> ⁴	PS	Awad (1994)
A1/2	Melut AY1/2	Sudan	10°34'37"N	33°05'56"E	Cretaceous	L Cretaceous	Maastrichtian	<i>Nypa</i>	PS	Eisawi (2007)
A3	Melut AY3	Sudan	09°45'33"N	33°11'44"E	Cretaceous	L Cretaceous	Maastrichtian	<i>Nypa</i>	PS	Eisawi (2007)
A4	Melut AY4	Sudan	08°34'00"N	33°45'36"E	Cretaceous	L Cretaceous	Maastrichtian	<i>Nypa</i>	PS	Eisawi (2007)
Gf	Gedaref	Sudan	14°01'28"N	35°22'07"E	Cretaceous	L Cretaceous	Maastrichtian	<i>Nypa</i>	PS	Eisawi & Schrank (2009)
HH	Hed Hed	Somalia	09°32'00"N	44°47'00"E	Cretaceous	L Cretaceous	Maastrichtian	<i>Nypa</i>	PS	Schrank (1990, 1994)
Fr	Foram 1	Egypt	27°38'42"N	25°12'21"E	Cretaceous	L Cretaceous	Maastrichtian	<i>Nypa</i>	PS	Schrank (1991)
Kg	Kharga	Egypt	25°26'21"N	30°33'31"E	Cretaceous	L Cretaceous	Maastrichtian	<i>Nypa</i>	PS	Schrank (1991, 1992)
Ab	Abu Gabra	Sudan	10°52'55"N	27°18'59"E	Cretaceous	L Cretaceous	Maastrichtian	<i>Nypa</i>	PS	Babikir (1997)
Md	Muglad	Sudan	11°02'05"N	27°44'57"E	Cretaceous	L Cretaceous	Maastrichtian	<i>Nypa</i>	PS	Eisawi et al. (2012)
										Kaska (1989)
Mt	Melut	Sudan	10°26'25"N	32°12'06"E	Cretaceous	L Cretaceous	Campanian	<i>Nypa</i>	PS	Eisawi & Schrank (2008)
							Maastrichtian			Kaska (1989)
As	Aswan	Egypt	23°39'08"N	32°11'27"E	Cretaceous	L Cretaceous	Campanian	<i>Nypa</i>	PS	Schrank (1992)
							Maastrichtian			
Kh	Kahraman	Egypt	30°52'42"N	26°36'53"E	Cretaceous	L Cretaceous	Campanian	<i>Nypa</i>	PS	Schrank & Ibrahim (1995)
							Maastrichtian			Abdel-Kireem et al. (1996)
Mm	El Mahamid	Egypt	25°24'02"N	32°35'51"E	Cretaceous	L Cretaceous	Campanian	<i>Nypa</i>	PS	Schrank (1992)
							Maastrichtian			

Ki	Bir Kiseiba	Egypt	22°40'17"N	29°54'31"E	Cretaceous	L Cretaceous	Campanian Maastrichtian	<i>Nypa</i>	PS	Schrank (1992)
Qs	Quseer/Kosseir	Egypt	26°05'05"N	34°16'49"E	Cretaceous	L Cretaceous	Campanian Maastrichtian	<i>Nypa</i>	PS	Schrank (1992)
Ff	Farafra	Egypt	27° 3'24"N	27°58'13"E	Cretaceous	L Cretaceous	Campanian Maastrichtian	<i>Nypa</i>	PS	Schrank (1991)
AG	Abu-Gharadig	Egypt	29°43'45"N	28°32'18"E	Cretaceous	L Cretaceous	Campanian Maastrichtian	<i>Nypa</i>	PS	Abdel-Kireem et al. (1996)
Sn	Shendi	Sudan	16°41'25"N	33°25'51"E	Cretaceous	L Cretaceous	Campanian Maastrichtian	<i>Nypa</i>	PS	Eisawi (2018)
At	Al-Fatk	Yemen	16°17'40"N	52°32'11"E	Cretaceous	L Cretaceous	Santonian Campanian	<i>Nypa</i>	PS	Alaug et al. (2013)
No	El-Noor	Egypt	31°19'35"N	26°04'19"E	Cretaceous	L Cretaceous	Turonian Coniacian	<i>Nypa</i> ⁵	PS	El-Soughier (2013)
Bh	Bahariya	Egypt	28°23'06"N	28°54'31"E	Cretaceous	L Cretaceous	Cenomanian	<i>Avicennia</i> ? ⁶	LF	Darwish & Attia (2007)
Sf	Safaniya	Saudi Arabia	27°56'16"N	48°39'39"E	Cretaceous	E Cretaceous	Albian	<i>Nypa</i> ?	PS	Srivastava (2000)

508
509
510
511
512
513

¹Identification doubtful (D.T. Pocknall, pers. comm.)

²Identification doubtful (Rull, 2025).

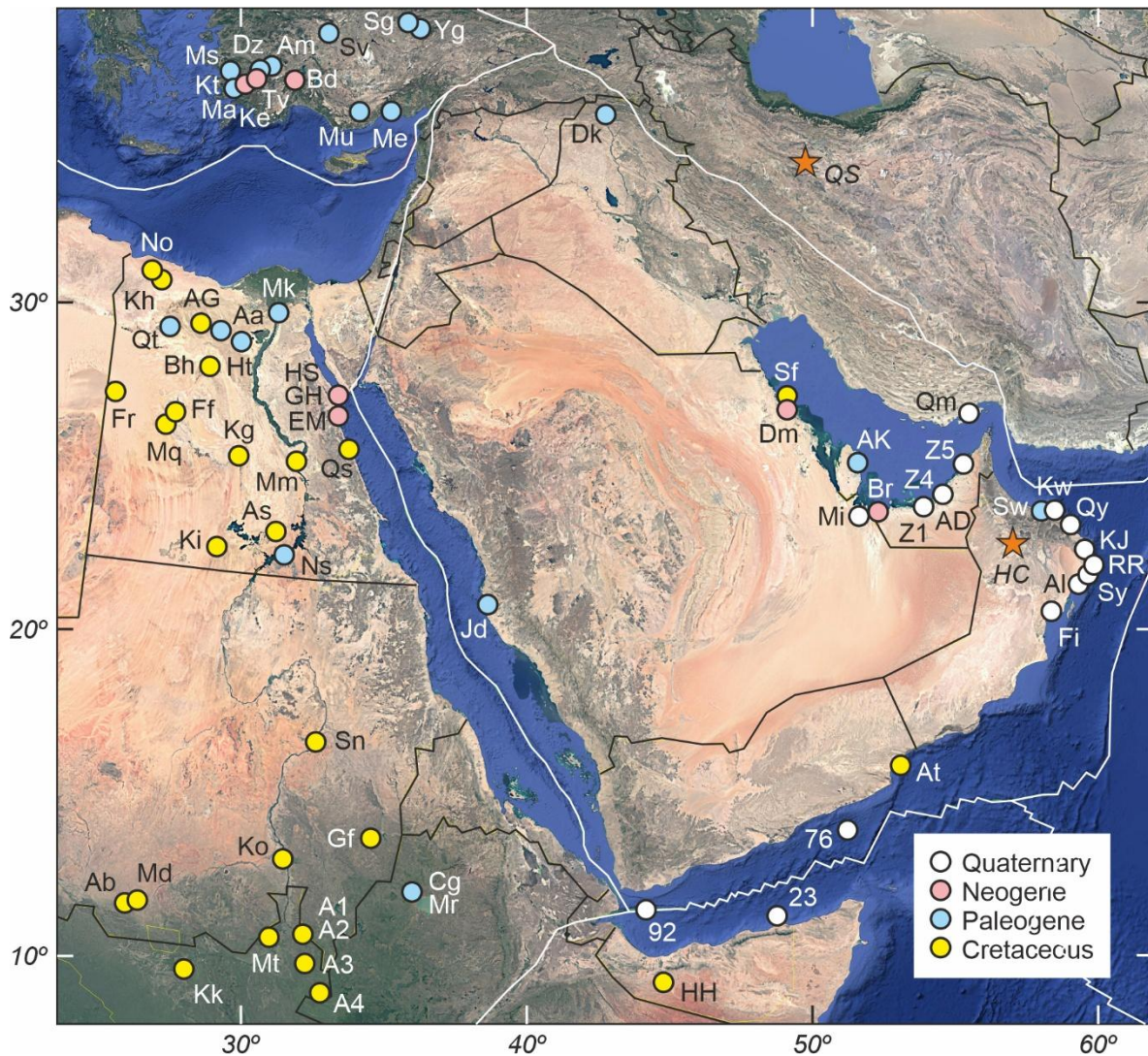
³Oldest macrofossil records worldwide (Wu et al., 2024).

⁴Identification doubtful (Pocknall et al., 2023).

⁵Wrong identification; the illustration provided corresponds to *Verrucatosporites*, a monoete spore.

⁶Identification considered as "highly speculative" (El Atfy et al., 2023a).

514



515

516

517

518

519

520

521

522

523

524

525

526

527

528

529

530

531

532

533

534

535

536

537

Figure 7. Localities with fossil records used in this review (see Table 2 for more details) using the same base map of Fig. 2. Orange stars represent the sites with paleoclimatic records discussed in the text (HC, Hoti Cave; QS, Qom section).

The presence of significant gaps in the palynostratigraphic record prompted the author to expand the search beyond conventional bibliographic and taxonomic resources by incorporating Google Search and AI tools such as ChatGPT and Gemini. As this expanded search failed to identify additional records, the resulting spatiotemporal gaps are more likely to reflect genuine absences of mangroves than deficiencies in information retrieval, although lack of research or unpublished records may contribute to the pattern in some areas.

4. Paleobiogeographical trends

This section uses the MESMA dataset to analyze biogeographical trends through time, which form the core of the review. It combines the fossil record with paleogeographical shifts derived from plate tectonics, along with independent paleoclimatic and paleoeustatic records, to investigate biogeographical shifts in terms of habitat suitability and the waxing and waning of dispersal pathways and barriers.

A previous comment on dispersal is pertinent. The colonization of new areas by a given taxon is usually referred to as dispersal *sensu lato*; however, in biogeography, it is useful to distinguish between long-distance dispersal (LDD) and migration. Here, the definitions proposed by Pielou (1979) are adopted. Long-distance dispersal, or jump dispersal, is the movement of organisms across great distances in short periods of time, usually shorter than the lifespan of an individual, and across inhospitable terrains. In

538 contrast, migration is a slower colonization process that occurs across hospitable terrains and lasts for
 539 generations (diffusion) or for sufficiently long periods to accommodate evolutionary change (secular
 540 migration). In the case of mangroves, long-distance dispersal involves intercontinental movement across
 541 oceans, with ocean currents acting as the main agents, whereas secular migration proceeds through the
 542 lateral expansion of populations via the progressive colonization of nearby habitats promoted by coastal
 543 currents (Van der Stocken et al., 2019).

544

545 4.1. Earliest potential Middle-East mangroves

546

547 Using the criteria established in this review—that is, the record of known mangrove taxa as presented in
 548 Table 1—the earliest consistent mangrove records correspond to the Late Cretaceous, specifically the
 549 Campanian–Maastrichtian (Table 2). However, some occasional earlier potential occurrences have been
 550 suggested and merit mention, one in the Albian and another in the Cenomanian.

551 The first reported potential mangrove element in the ME is monosulcate palm pollen of *Nypa*
 552 affinity from Albian sediments in the Persian Gulf (Srivastava, 2000). Pocknall et al. (2023) interpret this
 553 pollen as a potential *Nypa* ancestor and consider it the earliest known global record of this lineage. The
 554 significant spatial and temporal isolation of this finding—i.e., more than 1400 km from the nearest other
 555 Cretaceous mangrove occurrence (Fig. 7) and approximately 20–30 million years older than the
 556 Campanian–Maastrichtian—precludes any reliable assessment of the geographical patterns and temporal
 557 continuity of these potential mangrove occurrences in the region and globally. To date, the most
 558 parsimonious interpretation is to consider it a spatiotemporal outlier pending further research. If it is
 559 confirmed that this pollen represents a precursor of *Nypa*, the lineage would have evolved locally in the
 560 ME region.

561 The purported Cenomanian mangroves inferred from the fossil assemblage of the Bahariya Oasis
 562 in northern Egypt became iconic following the discovery of the giant sauropod dinosaur *Paralititan* (Smith
 563 et al., 2001). The site is now known as the mangrove-dinosaur site (Coiffard et al., 2025), and *Paralititan*—
 564 so named because of both its large size and its paralic habitat—is considered a unique dinosaur associated
 565 with mangrove environments. Mangrove conditions were inferred from the presence of the salt-tolerant
 566 tree-fern represented by *Weichselia reticulata* macroremains and from the sedimentological
 567 interpretation of low-energy littoral environments (Smith et al., 2001; Lacovara et al., 2003). Further
 568 investigations at the mangrove-dinosaur site also reported fossil leaves attributed to the well-known
 569 mangrove element *Avicennia* (Darwish & Attia, 2007; El-Saadawi et al., 2016). The Cenomanian Bahariya
 570 record is particularly significant because, if the paleoenvironmental interpretation is correct, it could
 571 represent the earliest mangrove community in the ME region. However, subsequent reassessments of the
 572 Bahariya record have challenged this interpretation.

573 Indeed, the mangrove affinity of *Weichselia* is not generally accepted, and the autecology of this
 574 extinct fern remains highly debated (Blanco-Moreno et al., 2018, 2020). Consequently, inferring mangrove
 575 ecosystems from its occurrence has been regarded as still speculative by El Atfy et al. (2023a). The same
 576 authors also questioned the identification of the fossil leaves attributed to *Avicennia*, considering this
 577 interpretation likewise highly speculative. *Avicennia* is not recorded in any other ME Cretaceous
 578 sediments, and its first appearances correspond to the Early Eocene (Table 2), close to the earliest global
 579 record, which dates to the Paleocene/Eocene boundary (Popescu et al., 2021).

580 More recent analyses of new samples (El Atfy et al., 2023b), together with reexaminations of
 581 previously collected fossil material (Coiffard et al., 2025), have adopted a more conservative approach to
 582 taxonomic assignment. Rather than assigning precise affinities, these studies use morphotypes to
 583 characterize the fossil assemblages and identify significant lateral and vertical variations that reflect
 584 complex spatiotemporal vegetation patterns, ranging from floodplain to coastal tropical humid
 585 environments within the Bahariya Formation. Therefore, based on the currently available evidence,
 586 interpreting the Cenomanian Bahariya Formation as a mangrove environment, and considering the giant
 587 *Paralititan* as a mangrove-dwelling dinosaur, appears premature. Unfortunately, this idea risks becoming
 588 established in the ME literature through repetition. *Weichselia* has also been reported from other ME
 589 localities (El-Khayal, 1985; Blanco-Moreno et al., 2018; El Atfy et al., 2023b), although no inferences
 590 regarding mangrove environments were made.

591 4.2. Late Cretaceous-Paleocene

592
593 During the Late Cretaceous, well before the collision between the Arabian and Eurasian plates,
594 southwestern Eurasia, extending from present-day Turkey to Iran, was covered by the Tethys Sea (Ali et
595 al., 2013; Moghadam et al., 2020), and land–sea transitional environments suitable for mangrove
596 development were absent from the region (Fig. 8). The present-day Arabian Peninsula, then still part of
597 the Nubian Plate, was emergent in its southwestern sector, corresponding to the Precambrian Arabian
598 Shield, whereas its northeastern sector was characterized by open to deep-marine environments, with
599 shallow-marine carbonate platforms bordering both Tethys coastal margins (Ziegler, 2001). Extensive
600 carbonate platforms are generally unfavorable for widespread mangrove development because they are
601 sediment-starved systems lacking a regular supply of terrigenous mud and stable fine-grained substrates
602 (Woodroffe et al., 2016; Breithaupt et al., 2017). Consequently, Late Cretaceous mangrove records are
603 restricted to the southwestern sector of the study area, primarily in northwestern Africa.

604 *Nypa* was the only mangrove component, and a large proportion of its records are from
605 continental areas. Extant *Nypa* requires a salinity range of 0‰ to 10‰ for optimal development, as
606 salinities exceeding 10‰ inhibit germination (Zhang et al., 2024). Therefore, it can be inferred that Late
607 Cretaceous ME *Nypa* grew preferentially in inland, and occasionally coastal, freshwater to brackish-water
608 environments. Interestingly, all *Nypa* localities are situated on the forefront of the Nubian–Arabian Plate,
609 whereas none occurs on the Eurasian side of the Tethys. The oldest purported *Nypa* record in the MESMA
610 dataset, identified as *Spinizonocolpites* in the original reference, comes from the Turonian–Coniacian of
611 Egypt (El-Soughier, 2013). However, the illustrated specimen assigned to *Spinizonocolpites* is actually a
612 monolete spore belonging to the form-genus *Verrucatosporites*, which has affinities with the
613 Polypodiaceae (Tryon & Lugardon, 1990). Therefore, the earliest confirmed *Nypa* record is from the
614 Turonian–Coniacian of Yemen (Alaug et al., 2013); all other records are Campanian–Maastrichtian in age
615 (Table 2).

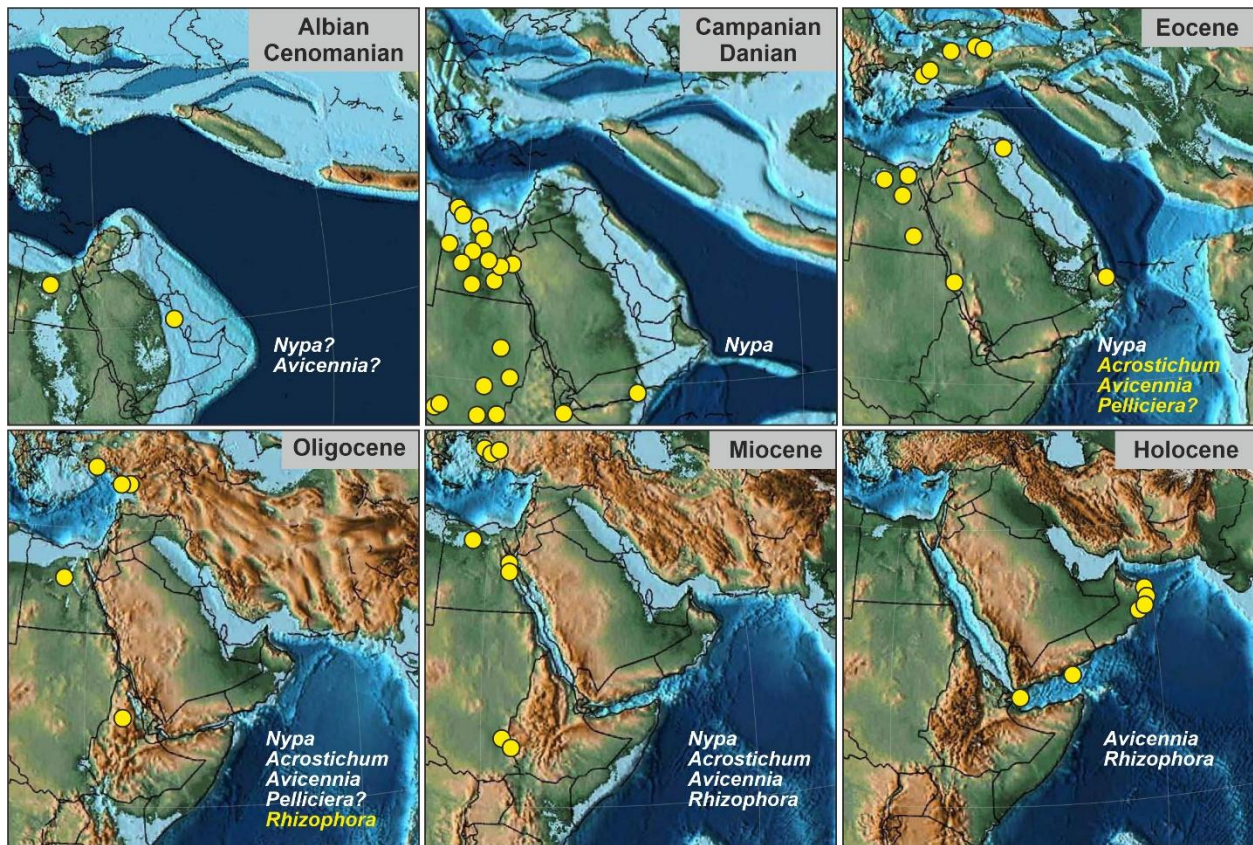
616 According to Muller (1981), *Nypa* appeared more or less simultaneously in South America, Africa
617 and Southeast Asia during the Late Cretaceous as a result of rapid invasion by seaborne dispersal across
618 the tropics. However, its geographical origin remains unknown. The Turonian–Coniacian record from
619 Yemen is currently the oldest documented Late-Cretaceous record worldwide. This, together with the
620 Albian record from Saudi Arabia discussed above, makes the ME region a strong candidate for the origin
621 of the *Nypa* lineage. This hypothesis is consistent with recent molecular phylogeographic studies (Wu et
622 al., 2024).

623 It is interesting to note that, although the Tethyan seaway remained open for dispersal through
624 either LDD, coastal migration, or both, Europe was devoid of mangroves during the Late Cretaceous and
625 the Paleocene (Rull, 2026). Therefore, the ME region emerges as a key area for the origin of mangroves
626 worldwide, whereas its role as a corridor for the dispersal of mangrove taxa from the IWP to Europe and
627 other regions developed later.

628 629 4.3. Eocene

630
631 A diversification of mangrove taxa occurred during the Eocene, with the establishment of *Avicennia*,
632 *Acrostichum*, and *Pelliciera*, although the occurrence of the latter has been questioned (Rull, 2025). These
633 taxa were recorded mainly in Turkey, with a single *Avicennia* record from Oman; the remaining records
634 correspond to *Nypa*, which remained dominant in the Nubian–Arabian Plate (Fig. 8). Most of the new
635 records were from the Tethyan coasts, suggesting that coastal migration from the IWP core was active by
636 this time. This diversification began during the Early Eocene Climatic Optimum (EECO) and the associated
637 sea-level rise, and continued throughout the Eocene (Fig. 9).

638
639

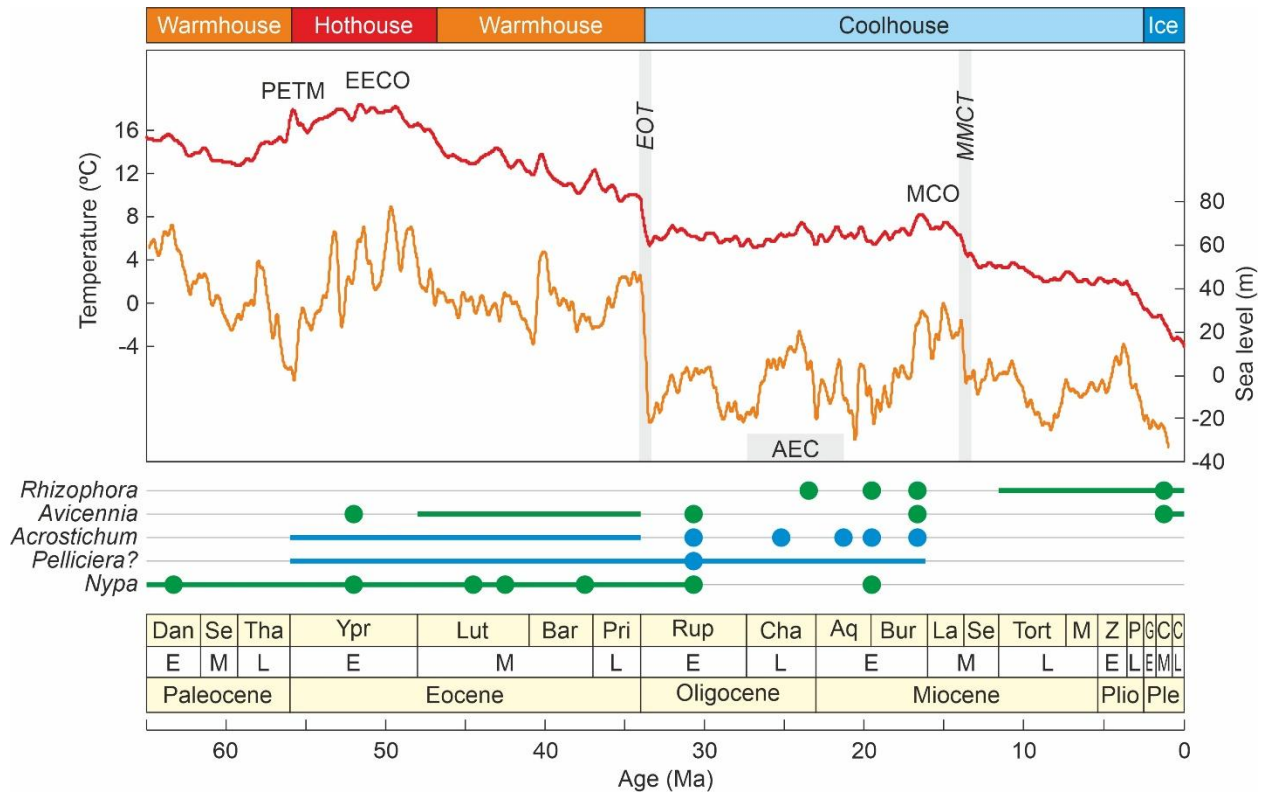


640
641
642 **Figure 8.** Paleobiogeographical trends of mangrove taxa from the Cretaceous to the Quaternary. Maps were generated with
643 GPlates 2.5.0 using the Scotese (2016) PALEOMAP PaleoAtlas, freely available at [https://www.earthbyte.org/paleomap-](https://www.earthbyte.org/paleomap-paleoatlas-for-gplates/)
644 [paleoatlas-for-gplates/](https://www.earthbyte.org/paleomap-paleoatlas-for-gplates/) (last accessed May 21, 2026).
645

646 Notably, other mangrove taxa, such as *Aegialitis*, *Aegiceras*, *Excoecaria*, Rhizophoraceae,
647 Sonneratiaceae and *Xylocarpus*, were already present in Europe by the Early-Middle Eocene (Rull, 2026),
648 suggesting that the ME region could have acted as a corridor for these taxa from the IWP core since the
649 Paleocene/Eocene boundary (P/E). The absence of these taxa in the ME region during the Eocene could
650 be due to local extirpation, although the lack of records discussed above may also have played a role. In
651 any case, the low diversity of mangrove taxa, compared with other IWP biogeographical provinces as
652 observed today (Saenger et al., 2019), seems to have originated long ago, at least by the early Paleogene.
653 This situation persisted throughout the Paleocene and Eocene, when a variety of global paleoclimatic and
654 paleoestatic changes took place (Fig. 9), and, based on the available evidence, cannot be linked to any
655 of these paleoenvironmental changes.

656 The possibility that LDD predominated over coastal migration would be consistent with this
657 pattern, at least in theory. However, the progressive shallowing of the Tethyan seaway and the resulting
658 expansion of coastal environments, together with the more or less continuous presence of *Acrostichum*,
659 *Avicennia* and *Nypa* along the Anatolian coasts (the proto-Mediterranean gateway to the European
660 domain), challenge this interpretation. The hypothesis of an early Paleogene colonization of the present-
661 day European continent by mangroves from the core IWP region via the ME Tethyan corridor is fully
662 consistent with the available paleobiogeographical evidence. However, the lack of fossil evidence
663 documenting such a process along the Tethyan coasts of both Europe and the ME represents a significant
664 knowledge gap that should be addressed by future research.
665
666
667
668
669
670

671



672

673

674 **Figure 9.** Chronostratigraphical ranges of mangrove taxa in the Middle East in relation to global paleoenvironmental
 675 reconstructions. Dots are records in particular time intervals and lines are records reported as ranges in the original literature.
 676 Major true-mangrove genera are in green and minor elements in blue. Global paleotemperature trends (red line) according to
 677 Wessterhold et al. (2021) and paleoeustatic trends (orange line) according to Miller et al. (2020). AEC, Arabia-Eurasia Collision;
 678 EECO, Early Eocene Climatic Optimum; EOT, Eocene/Oligocene Transition; MMCO, Middle Miocene Climatic Optimum; MMCT,
 679 Middle Miocene Climatic Transition; PETM, Paleocene/Eocene Thermal Maximum.

680

681 4.4. Oligocene

682

683 The maximum diversity of ME mangroves occurred during the Oligocene, with the addition of *Rhizophora*
 684 in an Egyptian locality, although the overall longitudinal extent of mangroves declined significantly (Fig.
 685 8). The environmental shift that most strongly affected other mangrove regions—namely, the cooling and
 686 eustatic sea-level fall associated with the Eocene/Oligocene Transition (EOT) (Fig. 9), which led to
 687 substantial diversity declines in Europe and the disappearance of *Nypa* from the Neotropics (Rull, 2023,
 688 2026)—does not appear to have affected ME mangroves in the same way. Similarly, the closure of the
 689 Tethyan seaway resulting from the Africa–Eurasia collision, which began during the Late Oligocene, was
 690 not associated with any decline in mangrove diversity or distribution. On the contrary, it coincided with
 691 the first appearance of *Rhizophora*. This suggests that *Rhizophora* had already crossed the Anatolian
 692 gateway before the closure of the Tethyan seaway, providing evidence for the progressive coastal
 693 colonization of the proto-Mediterranean region during the Paleogene. In summary, it is noteworthy that
 694 neither the EOT environmental disruption nor the closure of the Tethyan seaway—two key events in the
 695 evolution of mangroves elsewhere—were as influential for ME mangroves.

696

697 4.5. Miocene

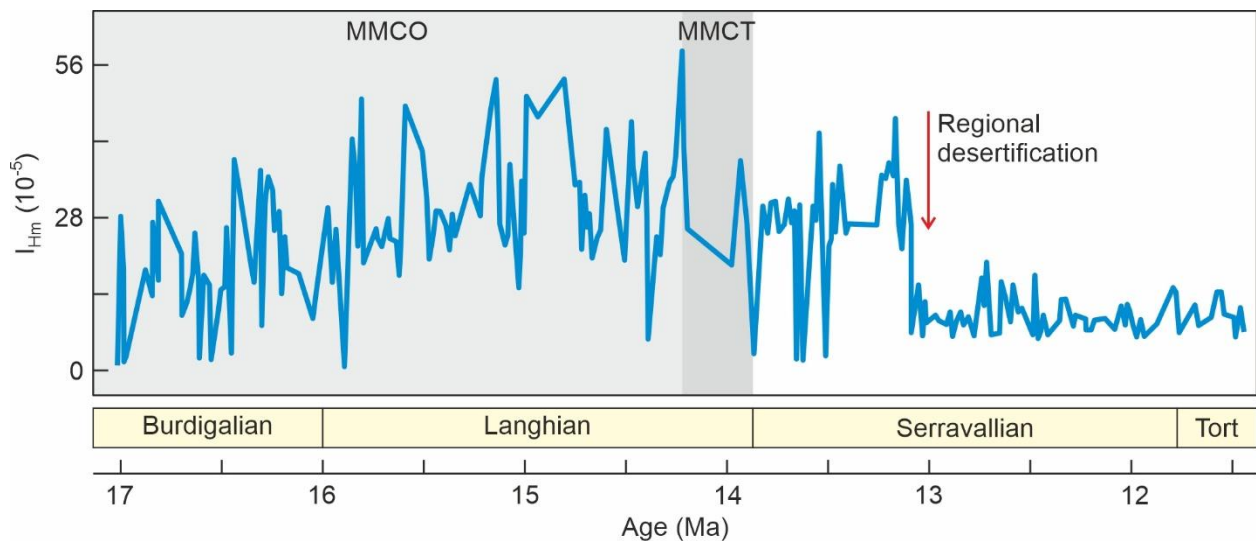
698

699 The main biodiversity crisis of ME mangroves took place during the Miocene, which witnessed the last
 700 occurrences of all mangrove taxa except *Rhizophora* and *Avicennia*, marking the beginning of the present-
 701 day situation. The last occurrences of *Nypa*, *Acrostichum*, and *Pelliciera* date from the Early Miocene,
 702 between the closure of the Tethyan seaway and the Middle Miocene Climatic Transition (MMCT) (Fig. 9).
 703 A clarification is warranted regarding *Nypa*, whose range extension into the Early Miocene is based on a

704 single occurrence from Egypt, extending its regional record by more than 10 million years beyond the EOT.
 705 However, the pollen illustration provided in support of this record does not appear to be consistent with
 706 *Nypa* and is more likely attributable to Malvaceae (D. T. Pocknall, pers. comm.), thus requiring further
 707 investigation. If this record is discounted, *Nypa* disappeared from the ME around the EOT, as it did in
 708 Europe and the Neotropics (Rull, 2023, 2026).

709 The MMCT occurred at approximately 14 Ma (14.2–13.8 Ma) and was characterized by global
 710 cooling, which has been linked to large-scale shifts in oceanic circulation associated with the progressive
 711 closure of the Tethyan seaway (Hamon et al., 2013). These changes led to decreased precipitation over
 712 North Africa and South Asia and have been interpreted as precursors to the development of modern
 713 desert systems (Zhang et al., 2023). In the Middle East, extensive aridification has been documented by
 714 approximately 13 Ma using independent physicochemical proxies (Sun et al., 2021; Xu et al., 2023) (Fig.
 715 10).

716



717

718

719 **Figure 10.** Middle–Late Miocene regional moisture changes reconstructed from magnetite-related sediment color properties in
 720 an outcrop of the Qom Formation (Iran) (Fig. 7). MMCO, Middle Miocene Climatic Optimum; MMCT, Middle Miocene Climatic
 721 Transition. Redrawn from Xu et al. (2023).

722

723 Therefore, the Miocene decline in mangrove diversity in the ME region, with *Avicennia* and
 724 *Rhizophora* as the only survivors, may be related to regional desertification, resulting in a situation that
 725 parallels present-day bioclimatic and biogeographical patterns. No Pliocene mangrove records were
 726 identified, and the occurrence of *Rhizophora* (Fig. 9) is based on a broadly dated Tortonian–Pleistocene
 727 record (Bonnefille, 2010).

728

729 4.6. Quaternary

730

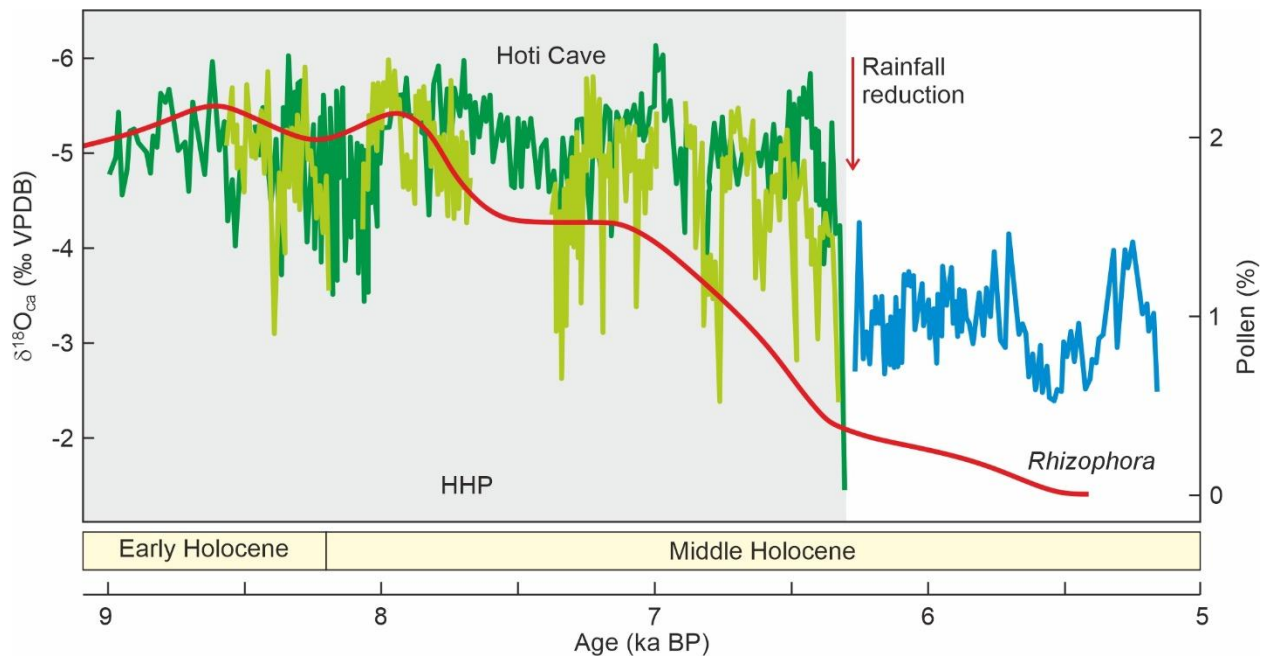
731 The Pleistocene is also nearly absent from the ME mangrove record, and virtually all sequences are
 732 Holocene and restricted to the southern and southeastern Arabian Peninsula (Fig. 7). These records
 733 contain only *Avicennia* and *Rhizophora*, and most are quantitative pollen records that enable detailed
 734 ecosystem reconstructions and comparisons with modern analogs. A characteristic feature of these pollen
 735 diagrams is a recurrent Middle Holocene decline in mangrove cover, inferred from pollen percentages,
 736 particularly for *Rhizophora*, whereas *Avicennia* remained stable or increased slightly. Currently,
 737 *Rhizophora* is absent from most Arabian mangroves, with only two exceptions along the Red Sea and Gulf
 738 of Oman coasts (Fig. 6). However, during the Early–Mid Holocene, this mangrove tree was more widely
 739 distributed and abundant, reaching pollen percentages of up to 40% (Lézine et al., 2017). The transition
 740 to the current situation occurred between 6.5 and 4.5 ka BP, depending on the site (Lézine, 2009; Lézine
 741 et al., 2002, 2010, 2017; Fersi et al., 2016).

742 Some authors consider this a general mangrove collapse event that began in the southern Arabian
 743 Peninsula at approximately 6 ka BP (Decker et al., 2020). There is no evidence that this event extended to

744 the entire ME region, but this possibility merits further investigation. Regarding the causes of this collapse,
 745 several explanations have been proposed, including climatic change, sea-level fluctuations and
 746 anthropogenic pressure. According to Decker et al. (2020), the most likely cause was a reduction in
 747 precipitation and the resulting increase in aridity, linked to a southward shift of the Intertropical
 748 Convergence Zone (ITCZ). These authors argue that Holocene climatic variability in Arabia was comparable
 749 to that observed in northern Africa, where a poleward shift of the ITCZ led to increased precipitation in
 750 the Sahara between approximately 11 and 6 ka BP during a phase known as the African Humid Period
 751 (AHP) (deMenocal & Tierney, 2012), followed by aridification and the establishment of the present-day
 752 desert conditions.

753 In the ME region, especially on the Arabian Peninsula, a similar Holocene Humid Period (HHP) has
 754 been identified, beginning at approximately 15 ka BP and gradually ending between 7.5 and 4 ka BP (Fersi
 755 et al., 2016). Subsequent paleoclimatic reconstructions based on independent physico-chemical proxies
 756 dated the termination of the HHP and the establishment of the current arid climate to approximately 6.3
 757 ka BP (Fig. 11) and supported a potential role for the southward migration of the ITCZ (Fleitmann et al.,
 758 2021). Within this generally accepted framework, local variations in the duration, intensity and underlying
 759 climatic mechanisms are possible (Enzel et al., 2015; Neugebauer et al., 2021). However, the chronological
 760 coincidence between the termination of the HHP and the Middle Holocene mangrove disruption strongly
 761 supports a potential causal connection.

762



763

764

765 **Figure 11.** Early–Middle Holocene moisture trends and *Rhizophora* pollen from the Arabian Peninsula. Moisture trends (blue-
 766 green tones) reconstructed from oxygen-isotope records in stalagmite calcite from Hoti Cave (Oman) (Fig. 7). Different colors
 767 represent different stalagmites from the same cave. *Rhizophora* pollen (red line) from site 92 (Yemen) (Fig. 7). HHP, Holocene
 768 Humid Period. Redrawn from Fleitmann et al. (2021) and Fersi et al. (2016).

769

770 The potential influence of aridification on the decline of *Rhizophora* (Fig. 11) and the persistence
 771 or expansion of *Avicennia* has been analyzed in light of the climatic and environmental niches of these
 772 mangrove-forming genera. Lézine (2009) and Lézine et al. (2010, 2017) emphasize that *Rhizophora* grows
 773 best in rainy tropical climates with abundant freshwater supply, and that its growth is inhibited by aridity,
 774 cool winter temperatures, and high salinity. In contrast, *Avicennia* tolerates a wider range of moisture and
 775 salinity conditions and is particularly adapted to hypersaline and evaporitic environments. These authors
 776 argue that the disappearance of *Rhizophora* and the persistence of *Avicennia* following the termination
 777 of the HHP suggest that a hydrological threshold was reached beyond which climatic conditions and
 778 freshwater availability were insufficient for *Rhizophora* to survive.

779 A more detailed characterization of the climatic niche of *Avicennia* showed that this taxon is highly
 780 tolerant of a wide range of temperature and moisture conditions and is limited only by winter frost, rather

This is a non-peer-reviewed preprint submitted to EarthArXiv

781 than by near-zero annual precipitation values (Quistoudt et al., 2012; Osland et al., 2017). Rull et al. (2026)
 782 considered the extant *Avicennia*-dominated mangroves of the Middle East to represent a latitudinal
 783 anomaly within the northernmost global belt of Northern Hemisphere mangroves, driven by climatic
 784 aridity and its associated ecophysiological consequences.

785 A word of caution is necessary here, as using a mangrove taxon as a straightforward climatic
 786 proxy, or as a component of a climatic index based on its known niche characteristics, may ultimately lead
 787 to circular reasoning. For example, Fersi et al. (2016) used the *Rhizophora* percentage curve as a proxy for
 788 humidity, whereas Lézine et al. (2017) introduced local and regional aridity indices based on the
 789 *Avicennia/Rhizophora* and *Artemisia/Rhizophora* ratios. These parameters may be useful for comparison
 790 with independent paleoenvironmental proxies, but they are unsuitable for investigating the response of
 791 vegetation, particularly mangroves, to paleoclimatic and paleoenvironmental changes. Sometimes,
 792 circularity may emerge unintentionally, as proxy-based reconstructions can propagate through the
 793 literature and become entrenched through repeated use, while their original formulation is gradually
 794 forgotten. This is why the risk is always present and should be continuously monitored.

795 Archaeological evidence shows that ancient societies used and managed mangroves and their
 796 associated terrestrial and marine resources (e.g., Berger et al., 2013). However, beyond local impacts,
 797 human activities do not appear to have substantially influenced mangrove diversity and biogeography at
 798 the regional scale. More recent historical and contemporary activities, such as coastal urbanization,
 799 aquaculture and oil pollution, have had a greater impact and have prompted conservation and restoration
 800 initiatives. The reader is referred to Meraj et al. (2025) for a comprehensive review.

801

802 5. Origin, dispersal and range shifts of individual taxa

803

804 The comparison of MESMA with CARMA, EURMA and other less structured datasets can be used to infer
 805 the spatiotemporal origins and dispersal/migration patterns of mangrove-forming taxa across the world's
 806 major mangrove regions. Considering the earliest fossil appearances of each major true-mangrove
 807 component (Table 3), the following patterns can be distinguished:

808

- 809 • *Caribbean origin*. Excluding doubtful identifications from Europe and the ME, *Pelliciera* is an exclusive
 810 AEP component that likely originated in the Caribbean during the Eocene. The occurrence of reliable
 811 records from western Africa ranging from the Eocene to the Miocene (Rull, 2025) suggests either a
 812 potential quasi-synchronous origin or a Caribbean origin followed by rapid migration to western
 813 Africa, always within the AEP region.
- 814 • *European origin*. The present European continent was the most probable origin of *Avicennia*, whose
 815 first appearance occurred at the P/E boundary. From there, *Avicennia* would have dispersed to the
 816 ME, likely through coastal migration, during the Early Eocene, and later to the Caribbean and
 817 southeastern Asia during the Miocene. These patterns are supported by recent molecular
 818 phylogenetic studies (Li et al., 2016; Takayama et al., 2021). Other Rhizophoraceae, such as *Bruguiera*
 819 and *Ceriops*, seem to follow similar Europe-centered patterns; however, their fossil record is still too
 820 scarce to support firm conclusions.
- 821 • *Middle East origin*. *Nypa* is usually considered to have appeared almost simultaneously across the
 822 pantropical zone during the Late Cretaceous (e.g., Muller, 1981; Gee, 2001; Srivastava & Prasad,
 823 2019). However, the discovery of a potential *Nypa* precursor in the ME, together with the suggestion
 824 of local evolution of this lineage in the study area, points to a possible ME origin followed by rapid
 825 eastward and westward dispersal worldwide. This ME-centered scenario is also supported by recent
 826 molecular phylogenetic studies (Wu et al., 2024).
- 827 • *SE Asia origin*. The earliest *Rhizophora* record dates from the Paleocene of southeastern Asia and
 828 dispersed, probably through a combination of migration and LDD, to Europe at the P/E boundary and
 829 to the Caribbean during the Middle to Late Eocene. Recent molecular phylogenetic studies also
 830 corroborate this view (Lo et al., 2014).
- 831 • *Unclear origin*. The case of *Sonneratia* is less clear, due to its almost simultaneous appearance in the
 832 Late Paleocene–Early Eocene in Europe and southeastern Asia, together with molecular phylogenetic
 833 studies indicating a Middle Eocene IWP origin (He et al., 2022).

This is a non-peer-reviewed preprint submitted to EarthArXiv

834
835
836 **Table 3.** Earliest fossil appearances of mangrove-forming tree genera (Table 1) shared among two or more major mangrove
837 regions worldwide at any time from the Late Cretaceous to the present. Although not a major component of extant mangroves,
838 *Pelliciera* is included because it was the dominant tree in Eocene Caribbean mangroves (Rull, 2022); however, the possibility of
839 misidentifications in Europe and the Middle East should be considered (Rull, 2025). Raw data are derived from comprehensive
840 compilations, namely CARMA (Rull, 2024), EURMA (Rull, 2026) and MESMA (this work) for the Caribbean, Europe and the Middle
841 East, respectively, and from Thanikaimoni (1978), Muller (1981) and Duke (2017) for southeastern Asia. Age assignments follow
842 the original reports. U, unreported in the region.
843

Genus	Caribbean (CARMA)	Europe (EURMA)	Middle East (MESMA)	SE Asia
<i>Avicennia</i>	Early-Middle Miocene	Paleocene/Eocene boundary*	Early Eocene	Early Miocene
<i>Bruguiera</i>	U	Early Eocene*	U	Late Miocene
<i>Ceriops</i>	U	Early Eocene*	U	Late Miocene
<i>Nypa</i>	Late Cretaceous*	Paleocene/Eocene boundary	Late Cretaceous*	Late Cretaceous*
<i>Pelliciera</i>	Early Eocene*	Paleocene/Eocene boundary ¹	Middle-Late Eocene ¹	U
<i>Rhizophora</i>	Middle-Late Eocene	Paleocene/Eocene boundary	Oligocene-Early Miocene	Paleocene*
<i>Sonneratia</i>	U	Paleocene/Eocene boundary*	U	Early Eocene

844 ¹Identification doubtful

845 *Oldest records worldwide

846
847 These preliminary inferences should be tested with the development of new regional datasets
848 (WAFMA and similar). For the time being, these proposals depict a spatiotemporally heterogeneous
849 biogeographical framework, which is more complex than the classical view of a more or less homogeneous
850 pantropical Late Cretaceous mangrove belt, subsequently differentiated by regional AEP/IWP
851 diversification after the emergence of the African barrier (Lo et al., 2014; Duke, 2017).

852 The widespread geographical distribution of *Nypa* during the Late Cretaceous and the Paleogene,
853 followed by its restriction to its present IWP range, is well known and has been attributed to
854 environmental factors, notably EOT cooling and sea-level fall (Gee, 2001; Pocknall et al., 2023; Rull, 2024).
855 This study provides additional data on the progression of this range contraction. Previous datasets
856 (CARMA and EURMA) recorded the last occurrences of *Nypa* at the Eocene/Oligocene boundary in the
857 Caribbean and in the Oligocene in Europe (Rull, 2024, 2026). In the ME, *Nypa* was also likely extirpated
858 during the EOT, unless a single Miocene record from Egypt is confirmed.
859

860 6. Mangroves as ecosystems

861
862 As emphasized in earlier reviews, a common misconception in mangrove research using fossils is the
863 inference of mangrove ecosystems from the occurrence of single mangrove taxa. This is the case, for
864 example, in the Late Cretaceous of the Caribbean region, which has been analyzed in detail by the author.
865 Until recently, the occurrence of Late Cretaceous mangroves in the Neotropics had been based solely on
866 *Nypa* records (e.g., Ellison et al., 1999; Srivastava et al., 2019). However, as shown by modern mangrove
867 ecology, these communities are defined by characteristic taxonomic, structural, and zonal features along
868 environmental gradients, notably topography, flooding, and salinity. Thus, a well-defined taxonomic
869 composition and clear zonation exist in Caribbean mangroves from the marine forefront to back-
870 mangrove brackish and freshwater environments, characterized by the succession *Rhizophora*–
871 *Avicennia*–*Pelliciera*–*Acrostichum*–*Mauritia*. Therefore, the identification of mangrove ecosystems in the
872 fossil record should be based on the occurrence of characteristic taxonomic assemblages associated with
873 environmental gradients.

874 Using these criteria, the first Caribbean mangroves as ecosystems were documented in the Middle
875 Eocene (>20 million years after the Cretaceous/Paleocene boundary) and were characterized by the
876 assemblage *Pelliciera*–*Nypa*–*Acrostichum*–*Mauritia* (*Rhizophora* and *Avicennia* had not yet reached the
877 region). This assemblage was consistent with a typical mangrove composition and a flooding/salinity
878 gradient (Rull, 2022). The earlier occurrence of *Nypa* alone since the Late Cretaceous was interpreted in
879 terms of brackish-water conditions—characteristic of *Nypa*, which does not tolerate normal marine
880 salinities (Zhang et al., 2024)—but it was considered insufficient to infer typical mangrove communities.

881 Therefore, it was proposed that the first Caribbean mangroves were not descendants of purported Late
 882 Cretaceous *Nypa* mangroves, but ecosystems that originated de novo in the Eocene (Rull, 2022).

883 This interpretation was made possible by the availability of quantitative pollen data—rather than
 884 presence/absence data alone, which represent another common limitation in deep-time paleontological
 885 research—which allow comparison with modern analogs. In Europe, similar quantitative studies have
 886 identified mangrove communities since the Paleocene/Eocene boundary, composed of *Nypa*, *Rhizophora*,
 887 *Sonneratia*, *Avicennia*, *Xylocarpus* and *Excoecaria*. *Nypa* has not been documented in the Cretaceous. In
 888 the ME, the situation is similar to that of the Caribbean, with numerous Late Cretaceous qualitative
 889 records of *Nypa*, but it differs in taxonomic diversity, with only two mangrove-forming taxa (*Rhizophora*
 890 and *Avicennia*) and in the scarcity of quantitative data. Therefore, the identification of mangrove
 891 ecosystems is more challenging. The first joint records of a characteristic forefront mangrove-forming
 892 taxon, *Avicennia*, and a typical back-mangrove component, *Nypa*, correspond to the Early Eocene of
 893 Oman. This could represent the first record of a true mangrove community in the region, but this should
 894 be confirmed with further research.

895

896 7. Conclusions

897

898 Based on the analysis of the MESMA dataset presented here, the following conclusions regarding the
 899 origin and development of ME mangroves can be advanced:

900

901 Origin. The earliest records of mangroves comparable to those of the present day correspond to *Nypa*
 902 and date from the Late Cretaceous. These records have been found on the northeastern Nubian Plate,
 903 along the southern shores of the Tethys Sea, well before the Arabian-Eurasian collision. A single older
 904 pollen record from the Early Cretaceous (Albian) is also available from the same region and may represent
 905 an ancestor of *Nypa*. If confirmed, this would constitute the earliest known record of the *Nypa* lineage
 906 and would suggest that the Middle East was the cradle of mangroves worldwide. Most Late Cretaceous
 907 *Nypa* records come from continental environments, consistent with the known ecological niche of extant
 908 *Nypa*, which inhabits freshwater to low-salinity brackish environments.

909

910 Diversification. ME mangroves did not diversify until the Eocene, with the arrival of *Avicennia*, probably
 911 from what is now Europe, and *Acrostichum*, whose geographical origin remains unknown. The occurrence
 912 of *Pelliciera* in the region has been called into question. This initial diversification coincided with the EECO,
 913 a phase characterized by the highest global temperatures and sea levels of the Cenozoic. Nevertheless,
 914 ME mangrove diversity remained substantially lower than in proto-Europe, which by that time harbored
 915 six additional true-mangrove elements. This is striking because the Tethyan seaway was likely the
 916 dispersal route between the IWP core area and Europe, yet no fossil evidence of this migration process
 917 has been found in the Middle East.

918

919 EOT resilience. Maximum diversity was attained during the Oligocene, at the onset of the Tethyan closure,
 920 following the addition of *Rhizophora*, likely originating from the IWP core region. This pattern contrasts
 921 with that observed in other mangrove regions, where the environmental disruption associated with the
 922 EOT led to significant reductions in mangrove distribution and biodiversity. As in Europe, *Nypa* appears to
 923 have survived across the EOT, although this inference is based on a single Miocene record of uncertain
 924 identification.

925

926 Neogene crisis. The first biodiversity crisis occurred during the Middle Miocene, when only two true
 927 mangrove components, *Avicennia* and *Rhizophora*, survived. This took place after the MMCT, a global
 928 climatic shift linked to changes in ocean circulation triggered by the closure of the Tethys Sea, whose
 929 manifestation in the Middle East was a regional desertification event that began around 13 Ma. Both the
 930 onset of regional desertification and the concomitant decline in diversity have been regarded as key
 931 precursors of the present-day situation.

932

933 Holocene crisis. A second bottleneck occurred much more recently, during the Middle Holocene, when
 934 *Rhizophora* underwent a marked decline and became restricted to a few sectors with suitable
 935 microenvironmental conditions. This paved the way for the modern ME mangrove configuration, with
 936 *Avicennia* as the dominant canopy-forming taxon. The decline of *Rhizophora* coincided with an
 937 aridification event that likely crossed a moisture threshold critical for its survival, as this genus requires
 938 humid climates and a stable freshwater supply for development. In contrast, *Avicennia* tolerates a wide
 939 range of precipitation regimes, including near-zero annual rainfall, as well as hypersaline waterlogged
 940 conditions.

941
 942 Biodiversity and biogeography. Considering the entire history of mangrove occurrence in the ME, this
 943 region contrasts with other mangrove-bearing regions worldwide in its low biodiversity, as only four
 944 genera of true mangroves (excluding the doubtful *Pelliciera* record) have been identified in the fossil
 945 record. Of these, one (*Nypa*) appears to have evolved locally, whereas another (*Avicennia*) likely dispersed
 946 from Europe and a third (*Rhizophora*) from Southeast Asia. The origin of the fourth, *Acrostichum*, remains
 947 uncertain. These features made the ME region more than merely a biogeographical corridor or barrier-
 948 switching zone, as it is often regarded in many studies.

949
 950 Mangrove ecosystems. Most pre-Quaternary fossil records in the MESMA dataset consist of qualitative
 951 presence/absence data, which complicates community reconstructions. If mangroves are considered
 952 well-structured ecosystems characterized by distinct taxonomic, architectural, and spatial patterns in
 953 relation to environmental gradients, the earliest mangrove communities appear to have emerged during
 954 the Early Eocene. This timing coincides with that previously documented in Europe and the Caribbean.

955

956 **8. Further research**

957

958 A remaining handicap for the study of ME mangroves is the presence of extensive spatiotemporal gaps in
 959 the fossil record. In some cases, these gaps have been attributed to the absence of a Late Cretaceous and
 960 Cenozoic stratigraphic record or to the unsuitability of rocks of these ages for preserving mangrove fossils
 961 due to environmental constraints. In other cases, however, suitable rocks are present, and the lack of
 962 records may reflect research biases or publication restrictions. Given the extensive development of the
 963 oil industry in the region and the importance of Cenozoic strata in petroleum systems, it is reasonable to
 964 assume that confidentiality issues may play a role.

965 A message to oil companies is that it is possible to contribute to scientific knowledge without
 966 compromising commercial competitiveness through agreed publication strategies. The Caribbean region,
 967 a cradle of palynostratigraphy applied to the oil industry, has provided many examples in this regard since
 968 the early development of the discipline, including publications such as Kuyl et al. (1955), Hopping (1967),
 969 Germeraad et al. (1968), Muller (1981), Lorente (1986) or Muller et al. (1987), among others – see Rull
 970 (2024) for a thorough compilation. A contribution of this kind from the Middle East would be not only
 971 very welcome but also widely recognized across all sectors, without implying any loss of competitiveness.

972 If the main information gaps can eventually be bridged, the following points, which have been
 973 highlighted throughout this paper, will require special attention:

974

- 975 • The possibility that the *Nypa* lineage evolved in the ME region, as suggested by the presence of a
 976 potential *Nypa* precursor in the Albian.
- 977 • The continental environments inhabited by Late Cretaceous–Paleocene *Nypa* populations in the
 978 northeastern Nubian Plate.
- 979 • The absence of fossil records of mangrove elements that were already present in Paleocene–Eocene
 980 Europe, despite their presumed dispersal/migration through the ME region.
- 981 • The taxonomic enrichment of ME mangroves during the EOT, a time of mangrove reduction and
 982 impoverishment in other mangrove-bearing regions worldwide.
- 983 • Whether *Nypa* persisted until the Miocene, as suggested by a single pollen record, or disappeared
 984 around the EOT, as occurred in Europe and the Caribbean.

- 985 • The reason why only *Avicennia* and *Rhizophora* survived the regional desertification that followed the
986 MMCT.
- 987 • The occurrence of Pliocene and Pleistocene mangroves and, if present, their composition and
988 geographical extent.
- 989 • Whether the so-called Middle Holocene mangrove collapse was restricted to the southern Arabian
990 Peninsula or extended across the entire ME region.
- 991 • The reason why *Rhizophora* endured the intense Pleistocene glacial–interglacial cycles but ultimately
992 succumbed to the Middle Holocene aridification event.
- 993 • In general, the reason for the low diversity of ME mangroves since their origin, compared with other
994 mangrove regions.

995

996 Finally, it is expected that the availability of new and more comprehensive information, both temporally
997 and spatially, will open new avenues of research that we cannot even foresee at present.

998

999

1000
1001
1002
1003
1004
1005
1006
1007
1008
1009
1010
1011
1012
1013
1014
1015
1016
1017
1018
1019
1020
1021
1022
1023
1024
1025
1026
1027
1028
1029
1030
1031
1032
1033
1034
1035
1036
1037

1038 **References**

- 1039
- 1040 Abdel-Fattah, Z.A., Gingras, M.K. 2020. Origin of compound biogenic sedimentary structures in the Eocene
1041 strata of Wadi El-Hitan universal heritage area, Fayum, Egypt: mangrove roots or not?
1042 Palaeogeography, Palaeoclimatology, Palaeoecology 560, 110048.
- 1043 Abdel-Kireem, M.R., Schrank, E., Samir, A.M., et al. 1996. Cretaceous palaeoecology, palaeogeography and
1044 palaeoclimatology of the northern Western Desert, Egypt. Journal of African Earth Sciences 22, 93-
1045 112.
- 1046 Abu El-Kheir, G.A.-M., Abdelgawad, M.K., Kassab, W.G. 2021. First known gigantic sea turtle from the
1047 Maastrichtian deposits in Egypt. Acta Palaeontologica Polonica 66, 349–355.
- 1048 Akkiraz, M.S., Kayseri, M.S., Akgün, F. 2008. Palaeoecology of coal-bearing Eocene sediments in Central
1049 Anatolia (Turkey) based on quantitative palynological data. Turkish Journal of Earth Sciences 17, 317–
1050 360.
- 1051 Akkiraz, M.S., Nazik, A., Ozgen-Erdem, N., et al. 2022. First micropalaeontological record from the early
1052 and middle Eocene Mamuca formation of the Dümrek Basin, western central Anatolia, Turkey:
1053 Biostratigraphy, depositional history and palaeoclimate. Journal of Asian Earth Sciences 224, 105036.
- 1054 Al-Atrush, A.H., Al-Hasson, A. 2025. Paleoeecology and paleoenvironment of the Middle-Late Eocene
1055 palynomorphs from the Gercus Formation, Duhok area, northern part of Iraq. Iraqi Geological Journal
1056 58, 227-237.
- 1057 Alaug, A.S., Batten, D.J., Ahmed, A.F. 2013. Organic geochemistry, palynofacies and petroleum potential
1058 of the Mukalla Formation (late Cretaceous), Block 16, eastern Yemen. Marine and Petroleum Geology
1059 46, 67-91.
- 1060 Alavi, M. 2007. Structures of the Zagros fold-thrust belt in Iran. American Journal of Science 307, 1064-
1061 1095.
- 1062 Ali, S.A., Buckman, S., Aswad, K.J., et al. 2013. The tectonic evolution of a Neo-Tethyan (Eocene-Oligocene)
1063 island arc (Walash and Naopurdan groups) in the Kurdistan region of the Northeast Iraqi Zagros
1064 Suture Zone. Island Arc 22, 104-125.
- 1065 Alsharan, A.S., Nairn, A.E.M. 1997. Sedimentary Basins and Petroleum Geology of the Middle East.
1066 Elsevier, Amsterdam.
- 1067 Awad, M.Z. 1994. Stratigraphic, palynological and paleoecological studies in the East-Central Sudan
1068 (Khartoum and Kosti Basins), Late Jurassic to Mid-Tertiary. Berliner Geowissenschaftliche
1069 Abhandlungen 161, 1-163.
- 1070 Babikir, A.E. 1997. Significance of the palynology and organic facies of the Abu Gabra No.1 well with
1071 respect to the petroleum geology of the Abu Gabra Field, Sudan. PhD dissertation, University of
1072 Southampton, UK.
- 1073 Berger, J.F., Charpentier, V., Crassard, R., et al. 2013. The dynamics of mangrove ecosystems, changes in
1074 sea level and the strategies of neolithic settlements along the coast of Oman (6000-3000 cal. BC).
1075 Journal of Archaeological Science 40, 3087-3104.
- 1076 Blanco-Moreno, C., Gomez, B., Buscalioni, A. 2018. Palaeobiogeographic and metric analysis of the
1077 Mesozoic fern *Weichselia*. Geobios 51, 571-578.
- 1078 Blanco-Moreno, C., Decombeix, A.-L., Prestianni, C. 2020. New insights into the affinities, autoecology,
1079 and habit of the Mesozoic fern *Weichselia reticulata* based on the revision of stems from Bernissart
1080 (Mons Basin, Belgium). Papers in Palaeontology 2020, 1-22.
- 1081 Bonnefille, R. 2010. Cenozoic vegetation, climate changes and hominid evolution in tropical Africa. Global
1082 and Planetary Change 72, 390-411.
- 1083 Bonnet, E. 1904. Sur un *Nipadites* de l'éocène d'Égypte. Bulletin du Museum d'Histoire Naturelle 10, 499-
1084 502.
- 1085 Bosworth, W. 2015. Geological evolution of the Red Sea: historical background, review, and synthesis. In
1086 Rasul, N.M.A. & Stewart, I.C.F. (eds.), The Red Sea. Springer, Berlin, pp. 45-78.
- 1087 Bosworth, W., Huchon, P., McClay, K. 2005. The Red Sea and Gulf of Aden basins. Journal of African Earth
1088 Sciences 43, 334-378.

- 1089 Breithaupt, J.L., Smoak, J.M., Rivera-Monroy, V.H., et al. 2017. Partitioning the relative contributions of
 1090 organic matter and mineral sediment to accretion rates in carbonate platform mangrove soils.
 1091 Marine Geology 390, 170-180.
- 1092 Bunting, P., Rosenqvist, A., Hilarides, L., et al. 2020. Global Mangrove Watch: updated 2010 mangrove
 1093 forest extent (v2.5). Remote Sensing 14, 1034.
- 1094 Celâl Şengör, A.M., Saniye, A. 2009. The Permian extinction and the tethys: an exercise in global geology.
 1095 Special Papers of the Geological Society of America 448, 1–106.
- 1096 Chandler, M.E.J. 1954. Some Upper Cretaceous and Eocene fruits from Egypt. Bulletin of the British
 1097 Museum (Natural History), Geology 2, 149-187.
- 1098 Chapman, V.J. 1976. Mangrove Vegetation. J. Cramer, Vaduz.
- 1099 Cohen, K.M., Finney, S.C., Gibbard, P.L., et al. 2013. The ICS international chronostratigraphic chart.
 1100 Episodes 36, 199–204.
- 1101 Coiffard, C., El Atfy, H., Darwish, M.H., et al. 2025. A reappraisal of the vegetation from the dinosaur-
 1102 bearing Bahariya Formation (lower Cenomanian; Cretaceous), Egypt. Swiss Journal of Palaeontology
 1103 144, 57.
- 1104 Cole, J.M., Abdelrahim, O.B., Hunter, A.W., et al. 2017. Late Cretaceous spore-pollen zonation of the
 1105 Central African Rift System (CARS), Kaikang Trough, Muglad Basin, South Sudan: angiosperm spread
 1106 and links to the Elaterates Province. Palynology 41, 547-578.
- 1107 Darwish, M. H., Attia, Y. 2007. Plant impressions from the mangrove dinosaur Unit of the Upper
 1108 Cretaceous Bahariya Formation of Egypt. Taekholmia 27, 105–125.
- 1109 Decker, V., Falkenroth, M., Lindauer, S., et al. 2020. Collapse of Holocene mangrove ecosystems along the
 1110 coastline of Oman. Quaternary Research 100, 52-76.
- 1111 deMenocal, P.B., Tierney, J.E. 2012. Green Sahara: African humid periods placed by Earth's orbital
 1112 cycles. Nature Education Knowledge 3, 12.
- 1113 Duke, N.C. 2017. Mangrove floristics and biogeography revisited: further deductions from biodiversity hot
 1114 spots, ancestral discontinuities, and common evolutionary processes. In: Rivera-Monroy, V.H., et al.
 1115 (eds.), Mangrove Ecosystems: A Global Biogeographic Perspective. Springer Nature, Cham, pp. 17-
 1116 53.
- 1117 Eisawi, A. 2007. Palynological and palaeoenvironmental interpretation of the Late Cretaceous to Tertiary
 1118 strata of the Melut Basin (southeast Sudan). PhD dissertation, Technische Universität Berlin,
 1119 Germany.
- 1120 Eisawi, A.A.M. 2018. Palynological evidence of a Campanian-Maastrichtian age of Shendi Formation,
 1121 Central Sudan. Africa Journal of Geosciences 1, 98-104.
- 1122 Eisawi, A., Schrank, E. 2008. Upper Cretaceous to Neogene palynology of the Melut Basin, Southeast
 1123 Sudan. Palynology 32, 101-129.
- 1124 Eisawi, A., Schrank, E. 2009. Terrestrial palynology and age assessment of the Gedaref Formation (eastern
 1125 Sudan). Journal of African Earth Sciences 54, 22-30.
- 1126 Eisawi, A.A.M., Ibrahim, A.B., Rahim, O.B.A., et al. 2012. Palynozonation of the Cretaceous to Lower
 1127 Paleogene strata of the Muglad Basin, Sudan. Palynology 36, 191-207.
- 1128 Ellison, A.M., Farnsworth, E.J., Merkt, R.E. 1999. Origins of mangrove ecosystems and the marine
 1129 biodiversity anomaly. Global Ecology and Biogeography 8, 95–115.
- 1130 El Atfy, H., Brocke, R., Uhl, D. 2013. Age and paleoenvironment of the Nukkul Formation, Gulf of Suez,
 1131 Egypt: insights from palynology, palynofacies and organic geochemistry. GeoArabia 18, 137-174.
- 1132 El Atfy, H., Brocke, R., Uhl, D. 2017. Palynology of the Miocene Rudeis and Kareem formations (Gharandal
 1133 Group), GH 404-2A Well, Gulf of Suez, Egypt. Abhandlungen der Senckenberg Gesellschaft für
 1134 Naturforschung 573, 1-134.
- 1135 El Atfy, H., El Beialy, S.Y., El Khoribi, E.M., et al. 2021. Continental palynomorphs from the Dabaa
 1136 Formation, North-Western Desert, Egypt: a contribution to the reconstruction of the vegetation on
 1137 the southern shores of the Tethys Ocean during the Early Oligocene. Botanical Journal of the Linnean
 1138 Society 197, 291-321.
- 1139 El Atfy, H., El Beialy, S.Y., Zobaa, M.K., et al. 2022. A snapshot into the Oligocene vegetation of the Tethyan
 1140 southern shores: new fossil pollen evidence from North Africa (Egypt). Palynology 46, 2023057.

- 1141 El Atfy, H., Coiffard, C., El Beilay, S.Y. 2023a. Vegetation and climate change at the southern margin of the
1142 Neo-Tethys during the Cenomanian (Late Cretaceous): Evidence from Egypt. PLoS ONE 18, e0281008.
- 1143 El Atfy, H., Coiffard, C., Uhl, D., et al. 2023b. A new florula dominated by angiosperms from the
1144 Cenomanian of Egypt. Cretaceous Research 149, 105554.
- 1145 El Beialy, S.Y. 1998. Stratigraphic and palaeoenvironmental significance of Eocene palynomorphs from the
1146 Rusayl Shale Formation, Al Khawd, northern Oman. Review of Palaeobotany and Palynology 102, 249-
1147 258.
- 1148 El Diasty, W.S., En Beialy, S.Y., Khairy, A., et al. 2020. Palaeoenvironmental and source rock potential of
1149 the Turonian-Miocene sequence in the West Esh El Mellaha (SW margin of the Suez rift, Egypt):
1150 insights from palynofacies, palynology and organic geochemistry. Review of Palaeobotany and
1151 Palynology 276, 104190.
- 1152 El-Hedeny, M., Kassab, W., Rashwan, M., et al. 2021. Bivalve borings in Maastrichtian fossil *Nypa* fruits:
1153 dakhla Formation, Bir Abu Minqar, South Western Desert, Egypt. Ichnos 28, 24-33.
- 1154 El-Khayal, A.A. 1985. Occurrence of a characteristic Wealden fern (*Weichselia reticulata*) in the Wasia
1155 Formation, central Saudi Arabia. Scripta Geologica 79, 75-88.
- 1156 El-Noamani, Z.M., Ziada, N.A. 2025. A juvenile *Nypa burtini* (Bronguiart) Ettingshausen from the early
1157 Eocene of southern Egypt. Taeckholmia 45, 56-69.
- 1158 El-Saadawi, W.E. 2005. A fossil rhizome at the mangrove site of Wadi Hitan, Egypt. Taeckholmia 25, 129-
1159 136.
- 1160 El-Saadawi, W., Osman, R., El-Faramawi, M.W., et al. 2016. On the Cretaceous mangroves of Bahariya
1161 Oasis, Egypt. Taeckholmia 36, 1-16.
- 1162 El-Saadawi, W., Osman, R., El-Paramawi, M., et al. 2018. On the Eocene mangroves of Wadi Al-Hitan World
1163 Heritage site, Fayum, Egypt. Egyptian Journal of Experimental Biology (Botany) 14, 197-209.
- 1164 El-Soughier, M.I. 2020. Paleoeological significance of palynomorphs from paleontologically-dated
1165 Maastrichtian-Danian deposits, Bir Abu Minqar area, South Western Desert, Egypt. Egyptian Journal
1166 of Geology 64, 423-431.
- 1167 El-Soughier, M.I. 2013. Palynology and palynofacies of the Upper Cretaceous succession of the El-Noor-
1168 1X borehole, northwestern Egypt. Arabian Journal of Geosciences 7, 1297-1311.
- 1169 El-Soughier, M.I., Mehrotra, R.C., Zhou, Z.Y., et al. 2011. *Nypa* fruits and seeds from the Maastrichtian-
1170 Danian sediments of Bir Abu Minqar, SouthWestern Desert, Egypt. Palaeoworld 20, 75-83.
- 1171 Enzel, Y., Kushnir, Y., Quade, J. 2015. The middle Holocene climatic records from Arabia: reassessing
1172 lacustrine environments, shift of ITCZ in Arabian Sea, and impacts of the southwest Indian and African
1173 monsoons. Global and Planetary Change 129, 69-91.
- 1174 Fersi, W., Lézine, A.M., Bassinot, F. 2016. Hydro-climate changes over southwestern Arabia and the Horn
1175 of Africa during the last glacial-interglacial transition: a pollen record from the Gulf of Ade. Review of
1176 Palaeobotany and Palynology 233, 176-185.
- 1177 Fest, B.J., Swearer, S.E., Arndy, S.K. 2022. A review of sediment carbon sampling methods in mangroves
1178 and their broader impacts on stock estimates for blue carbon ecosystems. Science of the Total
1179 Environment 816, 151618.
- 1180 Filatoff, J., Hughes, G.W. 1996. Late Cretaceous to Recent palaeoenvironments of the Saudi Arabian Red
1181 Sea. Journal of African Earth Sciences 22, 535-548.
- 1182 Fleitmann, D., Burns, S.J., Matter, A., et al. 2021. Moisture and seasonality shifts recorded in Holocene
1183 and Pleistocene speleothems from southeastern Arabia. Geophysical Research Letters 49,
1184 e2021GL097255.
- 1185 Fournier, M., Chamot-Rooke, N., Petit, C., et al. 2010. Arabia-Somalia plate kinematics evolution of the
1186 Aden-Owen-Carlsberg triple junction, and opening of the Gulf of Aden. Journal of Geophysical
1187 Research 115, B04102.
- 1188 Fraas, O. 1867. Geologisches aus dem Orient. Jahreshefte des Vereins für vaterländische Naturkunde in
1189 Württemberg 23, 145-148.
- 1190 Friis, G., Burt, J.A. 2020. Evolution of mangrove research in an extreme environment: historical trends and
1191 future opportunities in Arabia. Ocean & Coastal Management 195, 105288.

- 1192 García Massini, J.L., Jacobs, B.F., Pan, A., Tabor, N., Kappelman, J. 2006. The occurrence of the fern
1193 *Acrostichum* in Oligocene volcanic strata of the northwestern Ethiopian plateau. *International Journal*
1194 *of Plant Sciences* 167, 909-918.
- 1195 García Massini, J.L., Jacobs, B.F., Tabor, N.J. 2010. Paleobotany and sedimentology of Late Oligocene
1196 terrestrial strata from the northwestern Ethiopian Plateau. *Palaeontologia Electronica* 13, 1-51.
- 1197 Gee, C.T., Sander, P.M., Peters, S.E., et al. 2019. Fossil burrow assemblage, not mangrove roots:
1198 reinterpretation of the main whale-bearing layer in the late Eocene of Wadi Al-Hitan, Egypt.
1199 *Palaeobiodiversity and Palaeoenvironments* 99, 143-158.
- 1200 Germeraad, J.H., Hopping, C.A., Muller, J. 1968. Palynology of Tertiary sediments from tropical areas.
1201 *Review of Palaeobotany and Palynology* 6, 189-348.
- 1202 Ghandour, I.M., A-Zubieri, A.G., Basaham, A.S., et al. 2021. Mid-Late Holocene paleoenvironmental and
1203 sea level reconstruction on the Al Lith Red Sea Coast, Saudi Arabia. *Frontiers in Marine Science* 8,
1204 677010.
- 1205 Giraud, R., Bosworth, W. 1999. Phanerozoic geodynamic evolution of northeastern Africa and the
1206 northwestern Arabian platform. *Tectonophysics* 315, 73-104.
- 1207 Gregor, H.J., Hagn, H. 1982. Fossil fructifications from the Cretaceous–Palaeocene boundary of SW-Egypt
1208 (Danian, Bir Abu Munqar). *Tertiary Research* 4, 121–147.
- 1209 Hamon, N., Sepulchre, P., Lefebvre, V., et al. 2013. The role of eastern Tethys seaway closure in the Middle
1210 Miocene Climatic Transition (ca. 14 Ma.). *Climate of the Past* 9, 2687-2702.
- 1211 Hamzeh, M.A., Beni, A.N., Lahijani, H.A.K., et al. 2025. Mid- to Late-Holocene climate variability and
1212 mangrove development inferred from environmental shifts in the Gowatr Estuary on the Makran
1213 coast, northern Arabian Sea. *Palaeogeography, Palaeoclimatology, Palaeoecology* 661, 112714.
- 1214 Haseeba, K.P., Aboobacker, V.M., Vethamony, P., et al. 2025a. Significance of *Avicennia marina* in the
1215 Arabian Gulf environment: a review. *Wetlands* 45, 16.
- 1216 Haseeba, K.P., Aboobacker, V.M., Vethamony, P., et al. 2025b. Water and sediment characteristics in the
1217 *Avicennia marina* environment of the Arabian Gulf: a review. *Marine Pollution Bulletin* 216, 117963.
- 1218 He, Z., Xu, S., Zhang, Z., et al. 2020. Convergent adaptation of the genomes of woody plants at the land-
1219 sea interface. *National Science Review* 7, 978-993.
- 1220 Hesse, M., Zetter, R. 2007. The fossil pollen record of Araceae. *Plant Systematics and Evolution* 263, 93-
1221 115.
- 1222 Hopping, C.A. 1967. Palynology and the oil industry. *Review of Palaeobotany and Palynology* 2, 23-48.
- 1223 Hughes, G.W., Johnson, R.S. 2005. Lithostratigraphy of the Red Sea region. *GeoArabia* 10, 49-126.
- 1224 Ibrahim, M.I.A., Bassiouni, E., El-Ghareeb, R., et al. 2024. Environmental and vegetation dynamics through
1225 the Oligocene to Early Miocene of North Africa (Egypt). *Geobios* 82, 31-51.
- 1226 Jacobs, B.F., Tabor, N., Feseha, :, et al. 2005. Oligocene terrestrial strata of northwestern Ethiopia: a
1227 preliminary report on paleoenvironments and paleontology. *Palaeontologia Electronica* 8, 1-19.
- 1228 Kaska, H.V. 1989. A spore and pollen zonation of early Cretaceous to Tertiary nonmarine sediments of
1229 central Sudan. *Palynology* 13, 79-90.
- 1230 Kayseri-Özer, M.S. 2014. Spatial distribution of climatic conditions from the Middle Eocene to Late
1231 Miocene based on palynoflora in Central, Eastern and Western Anatolia. *Geodinamica Acta* 26, 122–
1232 157.
- 1233 Kenig, F., Huc, A.Y., Purser, B.H., et al. 1989. Sedimentation, distribution and diagenesis of organic matter
1234 in a recent carbonate environment, Abu Dhabi, U.A.E. *Advances in Organic Chemistry* 16, 735-747.
- 1235 Khanna, P., Petrovic, A., Ramdani, A.I., et al. 2021. Mid-Holocene to present circum-Arabian sea level
1236 database: investigating future coastal ocean inundation risk along the Arabian plate shorelines.
1237 *Quaternary Science Reviews* 261, 106959.
- 1238 Kirkham, A. 1998. A Quaternary proximal foreland ramp and its continental fringe, Arabian Gulf, UAE. In:
1239 Wright, V.P. & Burchette, T.P. (eds.), *Carbonate Ramps*. Geological Society London Special
1240 Publications 149, 15-41.
- 1241 Koeshidayatullah, A., Al-Ramadan, K., Collier, R., et al. 2016. Variations in architecture and cyclicity in fault-
1242 bounded carbonate platforms: Early Miocene Red Sea Rift, NW Saudi Arabia. *Marine and Petroleum*
1243 *Geology* 70, 77-92.

- 1244 Kopp, C., Fruehn, J., Flueh, E.R., et al. 2000. Structure of the Makran subduction zone from wide-angle and
1245 reflection seismic data. *Tectonophysics* 329, 171-191.
- 1246 Kräusel, R. 1939. Ergebnisse der Forschungsreisen Prof. E. Stromers in den Wüsten Ägyptens. IV. Die
1247 fossilen Floren Ägyptens 3. Abhandlungen der Bayerischen Akademie der Wissenschaften,
1248 Mathematisch-naturwissenschaftliche Abteilung 47, 6-140.
- 1249 Kräusel, R., Stromer, E. 1924. Ergebnisse der Forschungsreisen Prof. E. Stromers in den Wüsten Ägyptens.
1250 IV. Die fossilen Floren Ägyptens 1-3. Abhandlungen der Bayerischen Akademie der Wissenschaften,
1251 Mathematisch-naturwissenschaftliche Abteilung 30, 3-48.
- 1252 Kuyl, O.S., Muller, J., Waterbolck, H.T. 1955. The application of palynology to oil geology with reference
1253 to western Venezuela. *Geologie en Mijnbouw* 3, 49-76.
- 1254 Lacovara, K.J., Smith, J.R., Smith, J.B., et al. 2003. The Ten Thousand Islands coast of Florida: a modern
1255 analog to low-energy mangrove coasts of Cretaceous epeiric seas. In: Davis, R.A. (ed.), *Proceedings*
1256 *5th International Conference on Coastal Sediments*, Clearwater Beach, Florida, pp. 1773-1784.
- 1257 Lambeck, K. 1996. Shoreline reconstructions for the Persian Gulf since the last glacial maximum. *Earth and*
1258 *Planetary Science Letters* 142, 43-57.
- 1259 Lejal-Nicol, A. 1987. Flores nouvelles du Paleozoique et du Mesozoique d’Egypte et du Soudan
1260 septentrional. *Berliner Geowissenschaftliche Abhandlungen A* 75, 151–248.
- 1261 Lézine, A.-M. 2009. Timing of vegetation changes at the end of the Holocene Humid Period in desert areas
1262 at the northern edge of the Atlantic and Indian monsoon systems. *Comptes Rendus Geosciences* 341,
1263 750-759.
- 1264 Lézine, A.-M., Saliège, J.-F., Mathieu, R., et al. 2002. Mangroves of Oman during the Late Holocene:
1265 climatic implications and impact on human settlements. *Vegetation History and Archaeobotany* 11,
1266 221-232.
- 1267 Lézine, A.-M., Robert, C., Cleuziou, S., et al. 2010. Climate change and human occupation in the Southern
1268 Arabian lowlands during the last deglaciation and the Holocene. *Global and Planetary Change* 72,
1269 412-428.
- 1270 Lézine, A.-M., Ivory, S.J., Braconnot, P., et al. 2017. Timing of the southward retreat of the ITCZ at the end
1271 of the Holocene Humid Period in Southern Arabia: data-model comparison. *Quaternary Science*
1272 *Reviews* 164, 68-76.
- 1273 Li, X., Duke, N.C., Yang, Y., et al. 2016. Re-evaluation of phylogenetic relationships among species of the
1274 mangrove genus *Avicennia* from Indo-West Pacific based on multilocus analyses. *PLoS One* 11,
1275 e0164453.
- 1276 Lo, E.Y.Y., Duke, N.C., Sun, M. 2014. Phylogeographic pattern of *Rhizophora* (Rhizophoraceae) reveals the
1277 importance of both vicariance and long-distance oceanic dispersal to modern mangrove distribution.
1278 *BMC Evolutionary Biology* 14, 83.
- 1279 Lorente, M.A. 1986. Palynology and palynofacies of the Upper Tertiary of Venezuela. *Dissertationes*
1280 *Botanicae* 99, 1-222.
- 1281 Macgregor, D.S., Reeves, C.V. 2025. A paleotectonic atlas of the African Plate: Permian to Recent. *Journal*
1282 *of Petroleum Geology* 48, 231-279.
- 1283 McCoy, E.D., Heck, K.L. 1976. Biogeography of corals, seagrasses, and mangroves: an alternative to the
1284 center of origin concept. *Systematic Zoology* 25, 201–210.
- 1285 Meraj, G., Abouleish, M.Y., Ali, T., et al. 2025. Middle Eastern mangroves at the arid limit (Red Sea and
1286 Arabian/Persian Gulf): eco-biophysical dynamics, blue-carbon MRV, climate-risk pathways, and
1287 governance for resilient restoration – a comprehensive review. *Frontiers in Marine Science* 12,
1288 1695426.
- 1289 Miller, K.G., Browning, J.V., Schmelz, W.J., et al. 2020. Cenozoic Sea-level and cryospheric evolution from
1290 deep-sea geochemical and continental margin records. *Science Advances* 6, eaaz1346.
- 1291 Moghadam, H.S., Li, Q.-L., Stern, R.J., et al. 2020. The Paleogene ophiolite conundrum of the Iran-Iraq
1292 border region. *Journal of the Geological Society* 177, 955-964.
- 1293 Mohamed, L.H. 2026. Unlocking nature-based solutions for climate resilience: mangroves and Somalia’s
1294 nationally determined contributions. In: Droege, P. (ed.), *Urban Energy Transition. Cities and Regions*
1295 *for a Stable Climate*. Elsevier, Amsterdam, pp. 421-443.

- 1296 Moltzer, J.G., Binda, P.L. 1981. Micropaleontology and palynology of the middle and upper members of
 1297 the Shumaysi Formation, Saudi Arabia. *Bulletin of the Faculty of Earth Sciences* 4, 57–76.
- 1298 Moltzer, J.G., Binda, P.L. 1984. Age and Depositional Environment of the Middle and Upper Members of
 1299 the Shumaysi Formation, Saudi Arabia. *Annals of the Geological Survey of Egypt* 14, 269–278.
- 1300 Morley, R.J. 2000. *Origin and Evolution of Tropical Rain Forests*. John Wiley & Sons, Chichester.
- 1301 Muller, J. 1981. Fossil pollen records of extant angiosperms. *Botanical Review* 47, 1-140.
- 1302 Muller, J., Di Giacomo, E., van Erve, A. 1987. A palynological zonation for the Cretaceous, Tertiary, and
 1303 Quaternary of northern South America. *AASP Contributions Series* 19, 7-76.
- 1304 Nagelkerken, I., Blaver, S.J.N., Bouillon, S., et al. 2008. The habitat function of mangroves for terrestrial
 1305 and marine fauna: a review. *Aquatic Botany* 89, 155–185.
- 1306 Neugebauer, I., Dinies, M., Plessen, B., et al. 2022. The unexpectedly short Holocene Humid Period in
 1307 Northern Arabia. *Communications Earth & Environment* 3, 47.
- 1308 Osland, M.J., Feher, L.C., Griffith, K.T., et al. 2017. Climatic controls on the global distribution, abundance,
 1309 and species richness of mangrove forests. *Ecological Monographs* 87, 341-359.
- 1310 Pan, A.D., Jacobs, B.F., Dransfield, J., Baker, W.J. 2006. The fossil history of palms (Arecaceae) in Africa
 1311 and new records from the Late Oligocene (28-27 Ma) of north-western Ethiopia. *Botanical Journal of*
 1312 *the Linnean Society* 151, 69-81.
- 1313 Patlakas, P., Stathopoulos, C., Flocas, H., et al. 2019. Regional climatic features of the Arabian Peninsula.
 1314 *Atmosphere* 10, 220.
- 1315 Peña, S., Dash, A., Baby, G., et al. 2020. Modelling principal stress orientations in the Arabian Plate using
 1316 plate velocities. *Geological Society London Special Publications* 546, 193-214.
- 1317 Pielou, E.C. 1979. *Biogeography*. Wiley, New York.
- 1318 Pirouz, M., Avouac, J.-P., Hassanzadeh, J., et al. 2017. Early Neogene foreland of the Zagros, implications
 1319 for the initial closure of the Neo-Tethys and kinematics of crustal shortening. *Earth and Planetary*
 1320 *Science Letters* 477, 168-182.
- 1321 Plaziat, J.-C., Cavagnetto, C., Koeniguer, J.-C., et al. 2001. History and biogeography of the mangrove
 1322 ecosystem, based on a critical reassessment of the paleontological record. *Wetlands Ecology and*
 1323 *Management* 9, 161–179.
- 1324 Pocknall, D.T., Clowes, C.D., Jarzen, D.M. 2023. *Spinizonocolpites prominatus* (McIntyre) Stover & Evans:
 1325 Fossil *Nypa* pollen, taxonomy, morphology, global distribution, and paleoenvironmental significance.
 1326 *New Zealand Journal of Geology and Geophysics* 66, 558–570.
- 1327 Popescu, S.-M., Suc, J.-P., Fauquette, S., et al. 2021. Mangrove distribution and diversity during three
 1328 Cenozoic thermal maxima in the Northern Hemisphere (pollen records from the Arctic-North
 1329 Atlantic-Mediterranean regions). *Journal of Biogeography* 48, 2771–2784.
- 1330 Por, F.D., Dor, I., Amir, A. 1977. The mangal of Sinai: limits of an ecosystem. *Helgoländer wissenschaftliche*
 1331 *Meeresuntersuchungen* 30, 295-314.
- 1332 Quistoudt, K., Schmitz, N., Randin, C.F., et al. 2012. Temperature variation among mangrove latitudinal
 1333 range limits worldwide. *Trees* 26, 1919-1931.
- 1334 Racey, A., Goodall, J.G.S., Keen, M.C., et al. 2025. Palynology, micropaleontology and geochemistry of the
 1335 Eocene Rusayl Formation of Northern Oman. *Geological Society London Special Publications* 550,
 1336 273-309.
- 1337 Rull, V. 2002. High-impact palynology in petroleum geology: applications from Venezuela (northern South
 1338 America). *American Association of Petroleum Geologists Bulletin* 86, 279-300.
- 1339 Rull, V. 2022. The Caribbean mangroves: an Eocene innovation with no Cretaceous presursors. *Earth-*
 1340 *Science Reviews* 231, 104070.
- 1341 Rull, V. 2023. Eocene/Oligocene global disruption and the revolution of Caribbean mangroves.
 1342 *Perspectives in Plant Ecology, Evolution and Systematics* 59, 125733.
- 1343 Rull, V. 2024. *Origin and Evolution of Caribbean Mangroves. A Time-Continuum Ecological Approach*.
 1344 Springer Nature, Cham.
- 1345 Rull, V. 2025. A critical evaluation of fossil pollen records from the mangrove tree *Pelliciera* beyond the
 1346 Neotropics: biogeographical and evolutionary implications. *Review of Palaeobotany and Palynology*
 1347 335, 105299.

- 1348 Rull, V. 2026. Origin, evolution and decline of European mangroves: The Cenozoic paleobotanical record.
1349 Earth-Science Reviews 278, 105506.
- 1350 Rull, V., Vicente, A., Bouchal, J.M., Casanovas-Vilar, I. 2026. On the use of extant Middle-East mangroves
1351 as modern analogs for Miocene Mediterranean-Paratethyan mangroves. *Palaeobiodiversity and*
1352 *Palaeoenvironments*, doi 10.1007/s12549-025-00693-y.
- 1353 Sadooni, F.N., Al-Saad, H. 2012. Mangrove-bearing limestone from the Eocene Damman Formation,
1354 Arabian Gulf: implications for the mangrove dispersal controversy. *Carbonates and Evaporites* 27,
1355 243-250.
- 1356 Saenger, P. 2003. *Mangrove Ecology, Silviculture and Conservation*. Springer, Dordrecht.
- 1357 Saenger, P., Ragavan, P., Sheue, C.-R., et al. 2019. Mangrove biogeography of the Indo-Pacific. In: Gul, B.,
1358 et al. (eds.), *Sabkha Ecosystems*, Springer Nature, Cham, pp. 379-400.
- 1359 Schrank E. 1990. Upper Cretaceous coal-bearing sediments in northern Somalia: short note on
1360 palynological age and palaeoenvironment. *Berliner Geowissenschaftliche Abhandlungen A* 120, 633-
1361 638.
- 1362 Schrank, E. 1991. Mesozoic palynology and continental sediments in NE Africa (Egypt and Sudan) – a
1363 review. *Journal of African Earth Sciences* 12, 363-373.
- 1364 Schrank, E. 1992. Nonmarine Cretaceous correlations in Egypt and northern Sudan: palynological and
1365 palaeobotanical evidence. *Cretaceous Research* 13, 351-368.
- 1366 Schrank, E. 1994. Palynology of the Yesoma Formation in northern Somalia: a study of pollen, spores and
1367 associated phytoplakton from the Late Cretaceous Palmae Province. *Palaeontographica B* 231, 63-
1368 112.
- 1369 Schrank, E., Ibrahim, M.I.A. 1995. Cretaceous (Aptian-Maastrichtian) palynology of foraminifera-dated
1370 wells (KRM-1, AG-18) in northwestern Egypt. *Berliner Geowissenschaftliche Abhandlungen* 177, 1-
1371 44.
- 1372 Scotese, C.R. 2016. PALEOMAP Paleomap for GPlates and the PaleoData Plotter Program, PALEOMAP
1373 Project, doi 10.13140/RG2.2.34367.00166.
- 1374 Sembroni, A., Reitano, R., Faccenna, C., et al. 2024. The geologic configuration of the Zagros fold and
1375 thrust belt: an overview. *Mediterranean Geoscience Reviews* 6, 61-86.
- 1376 Smith, J.B., Lamanna, M.C., Lacovara, K.J., et al. 2001, A giant sauropod dinosaur from an Upper
1377 Cretaceous mangrove deposit in Egypt. *Science* 292, 1704-1706.
- 1378 Spalding, M.D., Fox, H.E., Allen, G.R., et al. 2007. Marine ecoregions of the world: a bioregionalization of
1379 coastal and shelf areas. *BioScience* 57, 573-583.
- 1380 Spalding, M., Kainuma, M., Collins, L. 2010. *World Atlas of Mangroves*. Routledge, London.
- 1381 Srivastava, S.K. 2000. Palaeogeography of some Neocomian-Albian pollen and their significance in the
1382 evolution of phytogeoprovinces around the Early Cretaceous Atlantic Ocean. In: Harley, M.M., et al.
1383 (eds.), *Pollen and Spores: Morphology and Biology*. Royal Botanic Gardens, Kew, pp. 451–466.
- 1384 Srivastava, S.K., Binda, P.L. 1991. Depositional history of the Early Eocene Shumaysi Formation, Saudi
1385 Arabia. *Palynology* 15, 47-61.
- 1386 Srivastava, J., Prasad, V. 2019. Evolution and paleobiogeography of mangroves. *Marine Ecology* 40,
1387 e12571.
- 1388 Stern, R.J., Johnson, P. 2010. Continental lithosphere of the Arabian Plate: a geologic, petrologic, and
1389 geophysical synthesis. *Earth-Science Reviews* 101, 29-67.
- 1390 Sun, J., Talebian, M., Jin, C., et al. 2021. Timing and forcing mechanism of the final Neotethys seawater
1391 retreat from Central Iran in response to the Arabia-Eurasia collision in the late early Miocene. *Global*
1392 *and Planetary Change* 197, 103395.
- 1393 Takayama, K., Tateishi, Y., Kajita, T. 2021. Global phylogeography of a pantropical mangrove genus
1394 *Rhizophora*. *Scientific Reports* 11, 7228.
- 1395 Tantawy, A.A., Keller, G., Adatte, T., et al. 2001. Maastrichtian to Paleocene depositional environment of
1396 the Dakhla Formation, Western Desert, Egypt: sedimentology, mineralogy, and integrated micro- and
1397 macrofossil biostratigraphies. *Cretaceous Research* 22, 795-827.
- 1398 Thanikaimoni, G. 1987. *Mangrove Palynology*. Institut Français de Pondichéry, Travaux de la Section
1399 Scientifique et Technique 24, 1-100.
- 1400 Tomlinson, P.B. 2016. *The Botany of Mangroves*. Cambridge University Press, Cambridge.

- 1401 Torfstein, A., Steinberg, J. 2020. The Oligo-Miocene closure of the Tethys Ocean and evolution of the
1402 proto-Mediterranean Sea. *Scientific Reports* 10, 13817.
- 1403 Tryon, A.F., Lugardon, B. 1990. *Spores of Pteridophyta*. Springer, New York.
- 1404 Van Campo, E., Duplessy, J.C., Rossignol-Strick, M. 1982. Climatic conditions deduced from a 150-kyr
1405 oxygen isotope-pollen record from the Arabian Sea. *Nature* 296, 56-59.
- 1406 Van der Stocken, T., Carroll, D., Menemenlis, D., et al. 2019. Global-scale dispersal and connectivity in
1407 mangroves. *Proceedings of the National Academy of Sciences USA* 116, 915–922.
- 1408 Van Steenis, C.G.G.J. 1962. The distribution of mangrove plant genera and its significance for
1409 palaeogeography. *Proceedings of the Koninklijke Nederlandse Akademie van Wetenschappen* 65,
1410 164–169.
- 1411 Waleed, T.A., Abdel-Maksoud, Y.K., Kanwar, R.S., et al. 2025. Mangroves in Egypt and the Middle East:
1412 current status, threats, and opportunities. *International Journal of Environmental Science and*
1413 *Technology* 22, 1225-1262.
- 1414 Ward, R.D., Friess, D.A., Day, R.H., et al. 2016. Impacts of climates change on mangrove ecosystems: a
1415 region by region overview. *Ecosystem Health and Sustainability* 2, 01211.
- 1416 Westerhold, T., Marwan, N., Drury, A.J., et al. 2020. An astronomically dated record of Earth’s climate and
1417 its predictability over the last 66 million years. *Science* 369, 1383–1387.
- 1418 White, J.M. 2008. Palynodata Datafile: 2006 version. Geological Survey of Canada, Open File 5793, Natural
1419 Resources Canada, doi 10.4095/225704 (<https://paleobotany.ru/palynodata>; last accessed May 10,
1420 2026).
- 1421 Whybrow, P.J., McClure, H.A. 1980/1981. Fossil mangrove roots and palaeoenvironments of the Miocene
1422 of the eastern Arabian Peninsula. *Palaeogeography, Palaeoclimatology, Palaeoecology* 32, 213-225.
- 1423 Wood, W.W., Bailey, R.M., Hampton, B.A., et al. 2012. Rapid late Pleistocene/Holocene uplift and coastal
1424 evolution of the southern Arabian (Persian) Gulf. *Quaternary Research* 77, 215-220.
- 1425 Woodrofe, C.D., Rogers, K., McKee, K.L., et al. 2016. Mangrove sedimentation and response to relative
1426 sea-level rise. *Annual Review of Marine Science* 8, 243-266.
- 1427 Wu, W., Feng, X., Wang, N., et al. 2024. Genomic analysis of *Nypa fruticans* elucidates its intertidal
1428 adaptations and early palm evolution. *Journal of Integrative Plant Biology* 66, 824-843.
- 1429 Xu, S., He, Z., Guo, Z., et al. 2017. Genome-wide convergence during evolution of mangroves from woody
1430 plants. *Molecular biology and Evolution* 34, 1008-1015.
- 1431 Xu, L., Sun, J., Talebian, M., et al. 2023. Evidence for enhanced aridification since 13 Ma in the Qom back-
1432 arc basin, Central Iran. *Palaeogeography, Palaeoclimatology, Palaeoecology* 629, 111784.
- 1433 Yilmaz, A.O. 2006. Coal potential of Turkey: coal and energy. *Energy Exploration and Exploitation* 24, 371-
1434 390.
- 1435 Zetter, R., Hesse, M., Frosch-Radivo, A. 2001. Early Eocene zona-aperturate pollen grains of the
1436 *Proxapertites* type with affinity to Araceae. *Review of Palaeobotany and Palynology* 117, 267-279.
- 1437 Zhang, J., Hu, Y., Zhu, C., et al. 2023. Modeling the effects of global cooling and the Tethyan Seaway closure
1438 on North African and South Asian climates during the Middle Miocene Climate Transition.
1439 *Palaeogeography, Palaeoclimatology, Palaeoecology* 619, 111541.
- 1440 Zhang, M., Zhong, C., Lv, X., et al. 2024. Germplasm resource status and seed adaptability of *Nypa fruticans*
1441 Wurmb, an endangered species in China. *Forests* 15, 1396.
- 1442 Zhao, Z., Hou, Z.-E., Li, S.-Q. 2022. Cenozoic Tethyan changes dominated Eurasian animal evolution and
1443 diversity patterns. *Zoological Research* 43, 3–13.
- 1444 Ziegler, M.A. 2001. Late Permian to Holocene paleofacies evolution of the Arabian Plate and its
1445 hydrocarbon occurrences. *GeoArabia* 6, 445-504.